January 2012

Enhancing the immune response through IKKbeta-induced activation of NF-kappaB

Emily Hopewell
University of South Florida, elhopewell@gmail.com

Enhancing the immune response through IKKβ-induced activation of NF-κB

by

Emily L. Hopewell

A dissertation submitted in partial fulfillment
of the requirements for the degree of
Doctor of Philosophy
Department of Cell Biology, Microbiology
and Molecular Biology
College of Arts and Sciences
University of South Florida

Major Professor: Amer A. Beg, Ph.D.

Date of Approval:
April 9, 2012

Keywords: adenovirus, vaccine, lung cancer, inflammation, immunity

Dedications

This dissertation is dedicated to my family, whose confidence has buoyed me throughout this journey. And to my two Marks--to my husband, Mark II, whose support and sense of humor has allowed me to keep sight of what is truly important. To my beautiful new son, Mark III, who has brought an eternal light to my heart.

Acknowledgements

I would first like to thank Dr. Amer Beg for his support and guidance as my mentor. I would also like to thank the members of my committee: Dr. Scott Antonia, Dr. Esteban Celis, Dr. Ken Wright, and Dr. Xue-Zhong Yu. Their input, advice, and reagents have been invaluable throughout my graduate career.

I would like to extend a special ‘thank you’ to Dr. Siddharth Balachandran for taking the time and making the effort to serve as my external dissertation committee chairperson.

A special ‘thank you’ is also extended to the Moffitt Core Facilities and their staff, whose expertise has improved my research and my knowledge. Also, to the Cell Therapies Core, who, although I did not use their resources for my research, gave me my start at Moffitt as a Medical Technologist Specialist. Their support is what propelled me into graduate school.

Finally, I would like to thank the past and present members of my lab: Xingyu Wang, Javier Valenzuela, Sofia Hussain, Junmei Wang, Weipeng Zhao, Michael and Chris Massengill, and Crystina Bronk. My graduate career would be much harder without their support and assistance.

Table of Contents

List of Tables

List of Figures

Abstract

Nuclear factor-κB (NF-κB) is one of the main regulators of inflammatory and immune responses. It is a family of transcription factors composed of five members: RelA, RelB, cRel, NF-κB1 (p105/p50), and NF-κB2 (p100/p52). Homo- and hetero-dimers of family members are inhibited by inhibitor of κB (IκB) family members and activated by IκB kinase (IKK) family members. The IKK family is comprised of IKKγ, IKKα, and IKKβ. The focus of my dissertation delves into the role of NF-κB activation by IKKβ in both an immunotherapy setting and its role in T cell mediated anti-tumor immune responses.

A central focus of immunotherapy is to develop vaccine adjuvants that are capable of enhancing a protective adaptive immune response. Microbial adjuvants in vaccines activate key transcription factors, including NF-κB and interferon response factors (IRF). The individual role of these transcription factors in successful vaccines is not clear. We used constitutively active IKKβ (CA-IKKβ) expressed in an adenoviral vector (AdIKK) to determine the role of classical NF-κB activation in a vaccine-induced immune response. In an *in vivo* model, AdIKK induced rapid and sustained NF-κB-driven inflammation in the lungs compared to the control virus. AdIKK infection had no impact on the magnitude of T cell activation as measured by IFN-γ production; however pulmonary inflammation

resulted in increased cellularity of draining lymph nodes (LN) at early timepoints resulting in increased early antibody and T cell responses. Taken together, these findings show that IKKβ-induced NF-κB activation of an inflammatory response affects the kinetics, but not the magnitude of the adaptive immune response.

NF-κB is activated in many tumor types and contributes to the progression of cancer by suppressing apoptosis, and enhancing proliferation, angiogenesis and metastasis. NF-κB is also activated in other cells within the tumor microenvironment and promotes inflammation initiated by neutrophils and macrophages. In addition to inflammatory cells, T cells can be found within the tumor microenvironment and are associated with improved patient survival. Using CA-IKKβ, we sought to determine if NF-κB activation in tumor cells could promote T cell mediated tumor immunity. In both primary tumors and a metastatic tumor model, we found that NF-κB expression in tumors rendered immunogenic through expression of Kb-OVA led to tumor rejection or growth suppression. Tumor regression was mediated by increased CD8 T cell recruitment by chemokines. Microarray results showed increases in T cell chemokines, including CCL2 and CCL5. Knock-down of CCL2 by Lentiviral shRNA in LLC-OVA-IKK cells resulted in abrogation of tumor regression. These results suggest that NF-κB is capable of promoting immune surveillance in tumors through increased recruitment of T cells.

Overall, my dissertation highlights beneficial roles of IKKβ-induced activation of NF-κB in two separate systems: vaccine induced immune responses and tumor immune surveillance.

Chapter 1. An introduction to innate immunity and NF-κB

1.1 Innate immunity

The immune system is comprised of a series of layered defenses. Each layer becomes increasingly more specific, starting from a non-specific general barrier such as the skin, down to receptors specific for just a few peptides in T cells. These various layers can be broken down into two groups: the innate immune system, and the adaptive immune system. Once microorganisms breech our physical barriers, the innate immune system becomes the first line of defense and is capable of initiating a rapid response. The innate immune system is responsible for activating the adaptive immune response, which is charged with generation of immunological memory. Cross-talk between these two systems is vital for a successful immune response.

1.1.1. The innate immune response

Once microorganisms break past our primary immune barriers, such as the skin and mucosal epithelium, the cells of the innate immune system become responsible for taking up the fight against the intruders. The cells that play a role in this fight include neutrophils, basophils, and eosinophils, collectively termed polymorphonuclear leukocytes (PMNs), macrophages, dendritic cells (DCs), and natural killer (NK) cells (1).

The cells in the innate immune system are capable of distinguishing self from non-self through pattern recognition receptors (PRRs) that recognize pathogen-associated molecular patterns (PAMPs) (2-4). PRRs function to activate complement, promote phagocytosis, and trigger the expression of inflammatory cytokines, chemokines, type I IFNs, and co-stimulatory molecules (1).

The best-studied PRR family is the Toll-like receptor (TLR) family. TLRs dictate specificity through their location and recognition of specific PAMPs. For instance, TLR4 recognizes LPS and is located on the cell surface, whereas TLR9 is located on the endosomal membrane and recognizes unmethylated CpG (5).

All TLRs contain a conserved Toll-IL-1R (TIR) domain at the carboxyl terminus located in the cytoplasm. The TIR domain is responsible for recruiting adaptors to the TLR that can initiate cascades to activate transcription factors. Virtually all TLRs activate key transcription factors, including NF-κB and interferon (IFN) response factors (IRF); which play an integral role in promoting the adaptive immune response (6).

While TLR family members recognize PAMPs on the cell surface or endosomal membrane, other PRRs recognize PAMPs found within the cytoplasm (4, 7, 8). Various cytoplasmic PRRs exist and they are generally organized into two subfamilies: nucleotide binding oligomerization domain-leucine rich repeat (NOD-LRR) proteins and caspase activation and recruitment domain (CARD)-helicase proteins (4).

Members of the NOD-LRR family of proteins are responsible for recognizing bacterial components within the cytoplasm. Two of the best-studied NOD-LRR proteins, NOD1 and NOD2, are also capable of activating NF-κB for the induction of pro-inflammatory cytokines (8, 9). Proteins in this family combine to form macromolecular complexes called inflammasomes that recognize danger-associated molecular patterns and initiate an inflammatory response.

The CARD-helicase proteins are responsible for recognizing dsRNA produced by viruses in the cytoplasm (10). Two members of this family include retinoic acid-inducible protein I (RIG-I) and melanoma differentiation-associated gene 5 (MDA5). These closely related proteins are activated by dsRNA produced by viruses and association with the adaptor protein interferon β promoter stimulator 1 (IPS-1) results in downstream activation of the NF-κB and IRF transcription factor families (4, 11, 12).

During an infection, ligation of PRRs on resident leukocytes or viral infected cells results in the production of inflammatory chemokines. Chemokines function to recruit additional leukocytes, such as neutrophils and macrophages, to the area to initiate an inflammatory response and phagocytose necrotic cell debris or microbes (13). Chemokines are also responsible for bringing T cells into contact with dendritic cells to either initiate an adaptive immune response, in the case of infection, or to initiate tolerance, in the case of self antigens (14). Our lab, and others, have shown that the transcription factor NF-kB is responsible for the activation of many chemokines, such as CXCL1, CXCL2, IL-8, CXCL10, CCL2, and CCL5 (15-17).

1.1.2. Dendritic cells: Linking innate and adaptive immunity

As mentioned above, the innate immune system consists of several different cells: neutrophils, basophils, and eosinophils, macrophages, dendritic cells (DCs), and natural killer (NK) cells (1).

Natural killer cells are unique among innate immune cells because they are capable of directly lysing cells by releasing perforin and granzyme once they are activated by type I IFN and interleukin (IL-12) (18). Neutrophils and macrophages function as phagocytes and are capable of engulfing and killing microbial pathogens. A second function of macrophages includes recognition of PAMPs (discussed above) and secretion of cytokines and chemokines to initiate inflammation. Like macrophages, DCs also recognize PAMPs; however, unlike macrophages, DCs are the only professional antigen presenting cell (APC) capable of activating naïve T lymphocytes (19-22). This unique ability makes DCs an important bridge between the innate immune response and the adaptive immune response.

Immature DCs (iDCs) act as watchdogs of the innate immune system. They constantly patrol peripheral tissues sampling antigens. In the immature state, they express low levels of major histocompatibility complex (MHC) and co-stimulatory molecules, but are highly phagocytic.

In the absence of danger signals, iDCs are responsible for inducing peripheral tolerance to self antigens (23). When danger signals are initiated through bacterial or viral products, iDCs process pathogen antigens and express them in complex with MHC molecules on the cell surface. These activated iDCs

then undergo maturation (19-21). Mature DCs migrate to the lymph nodes, increase the expression of co-stimulatory molecules (CD40, CD80, CD86), secrete inflammatory cytokines and up-regulate MHC-peptide complexes on their surface. Once DCs arrive at the lymph nodes, T cells can be fully activated. Activation of T cells by DCs is a three step process. First, T cell receptors (TCR) must recognize the MHC:peptide complex presented. Second, co-stimulatory molecules on the APC (CD80 and CD86) must bind CD28 expressed on the T cell. Finally, the APC must secrete cytokines to direct the maturation of the T cells (19, 20, 22, 23). Previous work in our lab has shown that the transcription factor NF-κB plays an integral role in the activation of T cells by DCs. NF-κB is required for expression of costimulatory molecules as well as pro-inflammatory cytokines produced by DCs (24).

1.2. An introduction to NF-κB

As a main regulator of many immunological processes, the transcription factor NF-κB has garnered the attention of many researchers in the past few decades. Since its discovery in 1986, over 40,000 articles have been published on the family. As the name suggests, it was first discovered as a protein in the nucleus of B cells that binds kappa light chain enhancer sequences (25). Since its initial discovery, research has shown that NF-κB is ubiquitously expressed and is capable of activating a wide range of genes with varying functions, from activation of the immune response to inhibition of apoptosis (26, 27) Due to its

broad and varied functions, NF-κB has been found to play a role in a myriad of human diseases, from autoimmunity to cancer (28-31).

1.2.1. The NF-κB family

The NF-κB family is comprised of 5 transcription factors: RelA (p65), RelB, cRel, NF-κB1 (p105/p50), and NF-κB2 (p100/p52) (Figure 1.1). All five members contain a highly conserved rel homology region (RHR) as well as a DNA binding domain (DBD) that allows DNA binding as well as dimerization with other family members and binding of the inhibitors of κB (IκB) (32). The active transcription factor exists as a dimer that is sequestered in the cytoplasm by inhibitors.

Three members of the family, RelA, RelB, and cRel, contain a transactivation domain on their carboxyl terminus and are capable of activating transcription when released from their inhibitors. Although these three factors are highly homologous, they have functional specificity, highlighted in previous genetic knockout studies (24, 33-36).

NF-κB1/p50 and NF-κB2/p52 have a transrepression domain instead of a transactivation domain; therefore they cannot activate transcription unless partnered with one of the other three family members. These two proteins must be processed through proteasomal degradation of their precursors (p105 and p100) before they can become activated. Homodimers of p50 or p52 typically act as repressors of transcription (37).

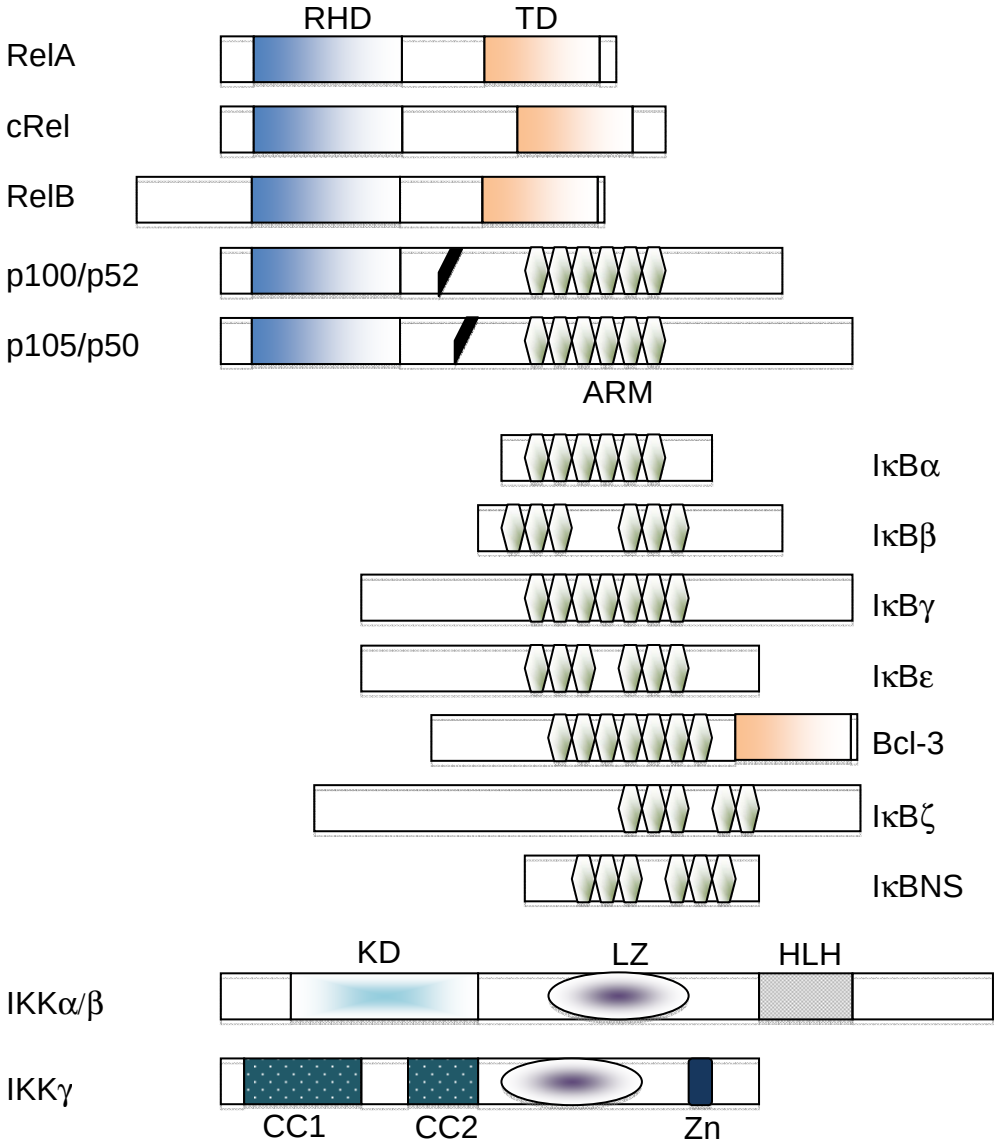

Figure 1.1. *The mammalian NF-κB and IκB families and IKK subunits.* Slashes show cleave site on p100 and p105 to generate p52 and p50. RHD: rel-homology domain. TD: transactivation domain. ARM: ankyrin repeat motif. KD: kinase domain. LZ: leucine zipper. HLH: helix-loop-helix. CC: coiled-coil. Zn: zinc finger.

1.2.2. Two pathways of activation

Activation of NF-κB can occur through two general pathways: the classical (Figure 1.2), and the alternative pathway (Figure 1.3). In a resting cell, NF-κB is sequestered in the cytoplasm by the inhibitors of kB (IκB). These proteins, along with NF-κB1 and NF-κB2, contain ankyrin repeat motifs (ARMs) that bind the RHR of NF-κB proteins. This binding masks the nuclear localization sequence, which sequesters NF-κB in the cytoplasm (38-40). Upon stimulation, NF-κB is released from IκB through activation of the IκB kinase (IKK) complex. Activation of the classical or the alternative pathway of NF-κB is dependent on the presence or absence of IKKγ (27, 41-43).

1.2.2a. The classical pathway

The classical pathway (Figure 1.2) is activated by stimuli such as ligation of TLRs, TNFR, or IL-1R and typically results in the activation of p50, RelA, and/or cRel and induction of inflammatory cytokines and chemokines such as IL-1β, TNFα, IL-6, IL-8, and KC (17). The IKK complex responsible for activation of the classical pathway is composed of the regulatory subunit IKKγ and two catalytic subunits, IKKα and IKKβ (44, 45) (Figure 1.1).

Upon stimulation, IKKβ is phosphorylated on serines 177 and 181 downstream of MAPK pathways and activates IKKβ allowing phosphorylation of IκB (46, 47). Phosphorylation of IκBα on serines 32 and 36 mark it for ubiquitination by the E3 ligase, β-TrCP/SCF and subsequent degradation by the 26S proteasome. Once IκB is released, NF-κB is free to translocate to the

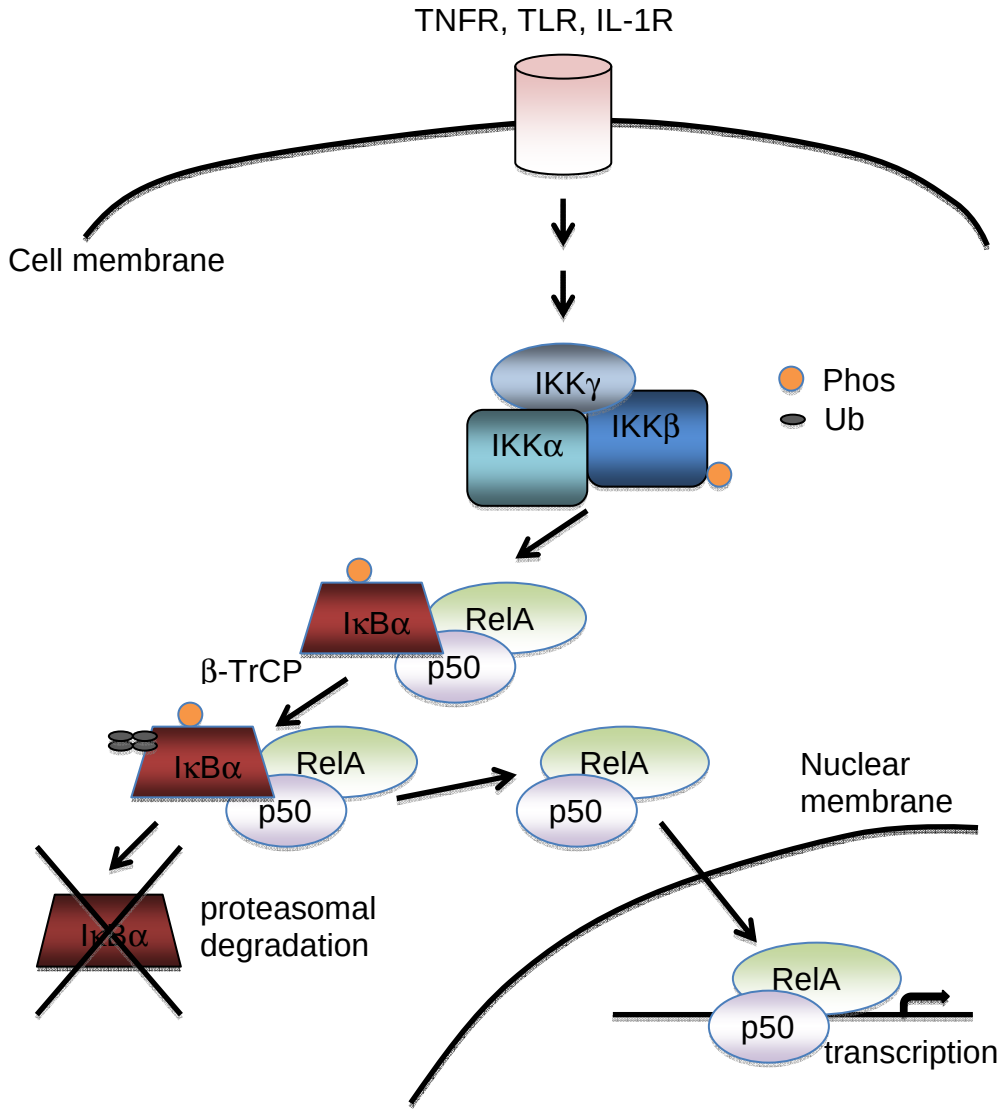

Figure 1.2. *The core classical NF-κB pathway.* Extracellular stimuli activate various pathways leading to the phosphorylation of IKKβ in the classical IKK complex. IKKβ phosphorylates IκB resulting in its ubiquitination by β-TrCP and degradation by the 26S proteasome. Freed NF-κB dimers, shown here as p50/RelA, translocate to the nucleus, bind κB sites and initiate gene transcription. Phos: phosphate, Ub: ubiquitin.

nucleus (26, 27, 37, 48). My research focused on the use of constitutively active IKKβ for activation of NF-κB in the immune response. IKKβ will be discussed further in section 2.3.

1.2.2b. The alternative pathway

The alternative pathway (Figure 1.3) is most commonly activated in response to members of the TNF superfamily, such as lymphotoxin β (49-51), CD40 (52), and B cell activating factor (BAFF) (53). Its activation is dependent on IKKα phosphorylation of NF-κB2/p100. This results in partial degradation of p100 to the active form, p52 and allows the p52/RelB complex to translocate to the nucleus (54, 55). The alternative pathway plays a part in adaptive immunity through its role in lymphoid organogenesis (34, 56, 57).

1.2.3. IKKβ

As discussed in section 2.2.1, the classical pathway of NF-κB activation hinges on phosphorylation of IKKβ. IKKβ was first discovered in 1997 (44) when it was teased out of the IKK signalosome identified in the previous year (58). The crystal structure of IKKβ was characterized in 2011 and differs somewhat from the accepted predicted structure (46, 59). Both the predicted and the crystalized structure of IKKβ contain a kinase domain on the amino terminus, and a NEMO (IKKγ) binding domain (NBD) on the carboxyl terminus; however, the crystal structure identifies a ubiquitin-like domain (ULD) and an α-helical scaffold/dimerization domain (SDD), which takes the place of the predicted leucine zipper (LZ) and helix-loop-helix (HLH) motifs. IKKβ interacts with IκBα through the ULD and SDD (59).

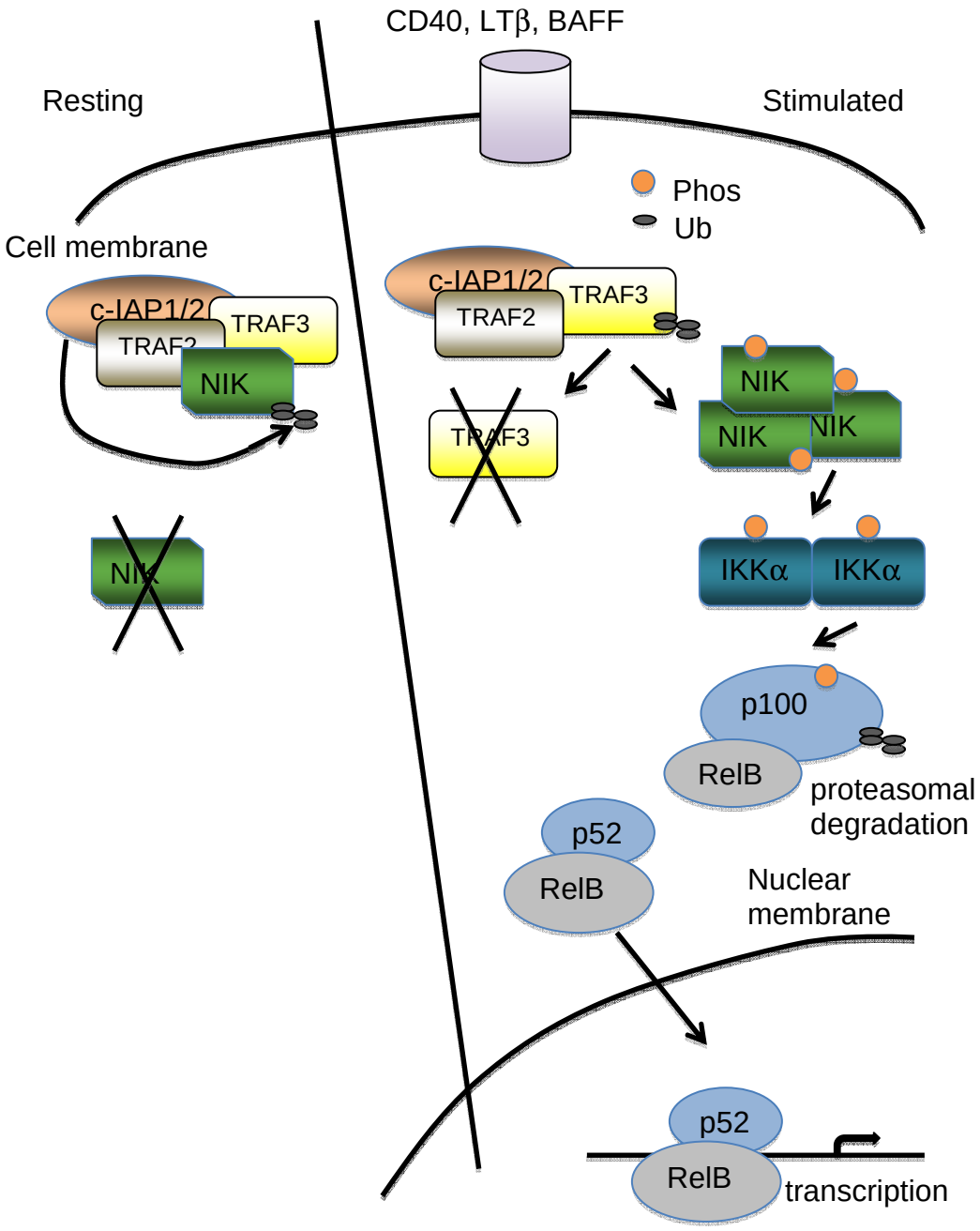

Figure 1.3. *The alternative NF-κB pathway.* In resting cells, NIK is ubiquitinated by c-IAP1/2, keeping NIK levels low. Upon stimulation, c-IAP1/2 ubiquitinates TRAF3, releasing NIK and allowing its accumulation and activation. Active NIK phosphorylates IKKα and IKKα can then phosphorylate p100, resulting in its processing to p52. Free p52/RelB can the translocate to the nucleus to induce target gene transcription. Phos: phosphate. Ub: ubiquitin.

Despite the discrepancy between the predicted and crystal structures, activation of IKKβ still requires phosphorylation of serines 177 and 181 within the kinase domain. How the phosphorylation of IKKβ occurs is still under discussion. The crystal structure of IKKβ, combined with knowledge garnered from previous crystal structures of IKKγ suggest that higher order oligomerization is responsible for trans-autophosphorylation (59). Mutation of serines 177 and 181 to glutamic acid produces a constitutively active form of IKKβ (CA-IKKβ). CA-IKKβ is sufficient for activation of classical NF-κB subunits (46); as such, it is a powerful tool for studying the activation of NF-κB in a variety of settings. Here, we have used CA-IKKβ to examine the role of IKKβ-induced NF-κB activation in a vaccine setting as well as in a tumor-induced immune response.

1.3. The role of NF-κB in vaccine-induced immunity

One of the many beneficial roles of NF-κB includes the induction of cytokines necessary to activate the adaptive immune response. During an infection, microbial adjuvants are recognized by dendritic cells (DCs) through pattern recognition receptors (PRRs) such as Toll-like receptors (TLRs) (4, 60, 61). TLR ligation results in the activation of key transcription factors, including NF-κB and interferon response factors (IRFs) (62).

It is widely believed that induction of a strong innate inflammatory response potentiates an adaptive immune response. In the case of a successful vaccine, microbial adjuvants also activate NF-κB and IRFs (63). This combined activation is responsible for the induction of the active form of IL-12 that can push

the immune response towards Th1-biased activation necessary for cell-mediated immunity (64); however, the individual roles of these transcription factors remains unclear.

Despite successes in limiting infectious diseases, vaccines for non-infectious diseases have fallen short. In the case of cancers, prophylatic or very early treatments have proven successful; yet this does not help the majority of cancer patients who typically present with well-established tumors. As such, a major goal of current immunotherapy is the development of strategies to treat established tumors (65-67). Before this can be done, a better understanding of what makes a successful vaccine is necessary.

One of the most common viral vectors used for immunotherapy are non-replicating adenoviruses (68-71). These viruses are in use in the clinic as stand-alone agents as well as viral vectors for DC vaccines (66, 71). These vectors are one of the most efficient vehicles for delivering genetic material to DCs with limited cellular toxicity. In DCs, adenoviral vectors induce maturation via an NF-κB-dependent pathway (72) and type I IFN signaling (73).

In chapter 2, we use an adenoviral vector to define the role of IKKβ-induced activation of NF-κB on the immune response to a virally encoded antigen. This approach gives us a clinically relevant model to examine and define the role of other activators of NF-κB and other transcription factors in a similar setting.

1.4. NF-κB in cancer

Very generally, cancer can be defined as uncontrolled cell growth. More specifically, Hanahan and Weinberg classified six hallmarks of cancer within the cell that dictate malignant growth. These alterations are: self-sufficiency in growth signals, insensitivity to anti-growth signals, evasion of programmed cell death (apoptosis), limitless replicative potential, sustained angiogenesis, and tissue invasion and metastasis (74). Inflammation has been suggested as a seventh hallmark of cancer (75-77).

Upregulation of NF-κB is present in many cancers, including lung cancer (78), melanoma (79), multiple myeloma (80), breast cancer (81), colorectal cancer (82), and lymphoma (83). NF-κB has been shown to play a role in at least some of the hallmarks of cancer, including self-sufficiency in growth signals, evasion of apoptosis, sustained angiogenesis, and invasion and metastasis (78, 79, 83-87). One of the most obvious links between NF-κB and cancer is the inhibition of apoptosis (88). In a normal cell, NF-κB regulates apoptosis by targeting genes such as Bcl-xL, inhibitors of apoptosis (IAPs), and c-FLIP.

A link between inflammation and cancer has been suspected since the 19th century when Virchow noted that inflammatory cells were present in tumor biopsies from patients (89). Prolonged inflammation, as well as exposure to carcinogens and inflammatory agents increase the risk of cancer (90-92). This link between inflammation and cancer has led many researchers to study the role of NF-κB in the tumor environment (31, 93-95).

NF-κB plays a role in the recruitment of tumor-promoting inflammatory cells, such as neutrophils and macrophages; however, NF-κB can also activate T cells and promote T cell-mediated tumor suppression (30). How can these two seemingly opposing functions of NF-κB be reconciled? Are they present in the same tumor, and what determines whether NF-κB activation in the tumor is good (immune promoting) or bad (tumor promoting)? Many questions about the function of NF-κB in immunogenic tumors still remain to be answered. In chapter 3, we attempt to shed a little light on this subject.

Chapter 2. IKKβ-induced inflammation impacts the kinetics but not the magnitude of the immune response to a viral vector

2.1. Abstract

Microbial adjuvants in vaccines activate key transcription factors, including NF-κB and interferon response factors (IRFs). However, the individual role of these transcription factor pathways in promoting adaptive immunity by adjuvants is not clear. It is widely believed that induction of a strong inflammatory response potentiates an adaptive immune response. In this study, we sought to determine whether activation of the pro-inflammatory inhibitor of κB kinase, IKK) canonical NF-κB pathway promoted vaccine-induced immune responses. An adenovirus expressing constitutively-activated IKKβ (AdIKK) induced robust DC maturation and high expression of key cytokines compared to a control virus. *In vivo*, AdIKK triggered rapid inflammation after pulmonary infection, increased leukocyte entry into draining LNs, and enhanced early antibody and T-cell responses. Notably, AdIKK did not influence the overall magnitude of the adaptive immune response. These results indicate that induction of inflammation by IKKβ/NF-κB in this setting impacts the kinetics but not the magnitude of adaptive immune responses. These findings therefore help define the individual role of a key pathway induced by vaccine adjuvants in promoting adaptive immunity.

2.2. Introduction

Despite the tremendous success of vaccines in limiting the spread of infectious diseases, the underlying mechanisms through which successful vaccines work are only beginning to be understood. A central focus of current research is to define innate immunity mediators that can function as adjuvants to enhance protective adaptive immunity (96). The discovery and utilization of novel adjuvants can be instrumental in enhancing vaccine efficacy against infectious agents and cancer (96, 97). Mammalian PRRs, including TLRs, induce intracellular signaling in response to a plethora of microbial agents resulting in induction of robust innate and adaptive immune responses (4, 60, 61). Specific TLR ligands therefore have efficacy as vaccine adjuvants (96). Two main classes of transcription factors are activated by virtually all TLR ligands: NF-κB and IRF (4, 98). However, the individual role of these transcription factor pathways in promoting immune response by vaccines is not clear. NF-κB plays a key role in regulating expression of genes involved in inflammation, innate and adaptive immunity (11, 24, 43, 99-104). NF-κB activation is mediated by IKKβ (the canonical pathway) and IKKα (the non-canonical pathway), both of which are regulated by NIK (17, 41, 105, 106). The goal of this study was to specifically define the role of the IKKβ canonical pathway in promoting vaccine-induced immune responses. We tested this in the context of an adenovirus vector, which are in clinical use as stand-alone vaccines (69, 70) and as antigen-expressing vectors for DCs (107).

2.3. Methods

2.3.1. Mice

Six to 8-week-old C57BL/6 mice were purchased from the National Cancer Institute (Frederick, MD). Six to 8-week-old Balb/C mice were purchased from Harlan Laboratories (Indianapolis, IN). OT-1 and OT-II mice were purchased from Jackson Laboratories (Bar Harbor, ME) and were bred at our animal facility. Mice were housed at the Comparative Medicine Facility at the Moffitt Cancer Center and Research Institute. p50-/-cRel-/- and RelA-/- have been described previously and were bred in-house (108). IFNAR-/- mice were kindly provided by Dr. Esteban Celis (Moffitt Cancer Center). NF-κB-luciferase mice were kindly provided by Dr. Noreen Luetteke (Moffitt Cancer Center). All colonies were maintained under specific pathogen free conditions. All experiments were performed following the guidelines of the Moffitt Cancer Center and the University of South Florida Institutional Animal Care and Use Committee.

2.3.2. Cell culture

293T cells were cultured in DMEM/10% FBS supplemented with 2 mM L-glutamine and antibiotics. AD-293 cells were purchased from Stratagene (Santa Clara, CA) and were cultured in 293T medium supplemented with 1 mM sodium pyruvate.

Bone marrow-derived dendritic cells (BMDC) were made from BM suspensions flushed from femurs and tibias of mice. Briefly, cells were cultured in 24-well plates in RPMI-1640 supplemented with 5% fetal bovine serum,

antibiotics, L-glutamine, and 2-ME in the presence of supernatant (3% vol/vol) from J558L cells transduced with murine GM-CSF at a density of $1x10^6$ cells/ml. DC clusters were harvested after 6 days of cultures and transferred to new 24-well plates at a density of $1\text{-}2x10^6$ cells/ml. DC generated were >95% $CD11c^+$. For antigen stimulation, DC were pulsed with OVA peptide (SIINFEKL) overnight prior to infection. For injection, DC were harvested 48h after infection and injected subcutaneously or intravenously.

Human peripheral blood mononuclear cells (PBMCs) were isolated normal donor buffy coats (Florida Blood Services) as described (109) with minor changes. Cells were cultured at $4\text{-}5.5x10^6$ cells/ml in complete medium supplemented with 5 ng/ml of GM-CSF and IL-4. Additional growth factors were added on day 3 and monocyte-derived dendritic cells (MoDCs) were harvested on day 5.

2.3.3. Adenovirus production and infection

Replication deficient AdGFP and AdIKK were purchased from Vector Biolabs. AdIKK was produced by cloning IKKβEE into the DUAL-GFP-CCM shuttle vector. Adenovirus stocks were amplified by serial culture in AD-293 cells. Virus was harvested from AD-293 cells using 4 freeze-thaw cycles in a dry ice/ethanol bath and a 37ºC water bath with vortexing between each cycle. Virus was purified and concentrated via CsCl density centrifugation after 3-4 rounds of amplification. Virus titers were determined using QuickTiter™ Adenovirus Titer Immunoassay Kit (Cell Biolabs, San Diego, CA) according to manufacturer's instructions. All purified virus stocks were tested for the presence of endotoxin

using the Limulus Amebocyte Lysate Assay with a sensitivity of 0.03 EU/ml (Associates of Cape Cod, East Falmouth, MA) using 10-fold serial dilutions of the virus. All stocks were negative for endotoxin at the 1:100 dilution.

HEK-293T cells were infected with adenovirus for 48 hours. BMDCs were infected with AdIKK or AdGFP on day 7 of culture for 48 hours. MoDCs were infected on day 5 of culture at an MOI of 500 in a minimal volume for 3 hours with occasional shaking, then cells were plated and cultured for 48 hours prior to analysis. Mice were given adenovirus subcutaneously in four sites for each mouse: each flank, tail base and scruff, or intratracheally. Intratracheal administration was performed under anesthesia with 3-5% Isoflurane. Mice were secured in a supine position on an incline of 30-45º, and the larynx was visualized with an otoscope. Upon visualization, 50 μl of virus was administered into the trachea using a catheter. Mice were euthanized by CO_2 inhalation.

2.3.4. Flow cytometric analysis

Uninfected (PBS), AdGFP, and AdIKK infected cells were collected and incubated in PBS/0.5% bovine serum albumin with anti-CD16/CD32 for five minutes at room temperature (RT) to inhibit Fc binding of antibodies. Then cells were stained with antibodies to CD11c-, B7.1-, B7.2, MHC I (H2K)-, MHC II (IA)- or ICAM 1-PE for 20 minutes on ice. All mouse and human antibodies were purchased from BD Biosciences-Pharmingen (San Diego, CA). Human MoDC were gated on Lin negative, HLA-DR positive populations. Flow cytometric analysis was performed on an LSR II cytometer (BD Biosciences, San Jose, CA). Aggregates and dead cells were excluded from analysis (110). Data were

acquired using CellQuest software (BD Biosciences, San Jose, CA) and analyzed using FlowJo software (Tree Star, Ashland, OR).

2.3.5. T cell proliferation

CD8 T cells were purified from OT-I transgenic mice by negative selection using antibodies to CD4, CD11b, CD11c, CD19, CD45R, CD49b, CD105, Anti-MHC-class II, and Ter-119 according to the manufacturer's instructions (Miltenyi Biotec, Auburn, CA). DC were pulsed with OVA (257-264) peptide (SIINFEKL) overnight and then infected with AdGFP or AdIKK for 48 hours. CD4 T cells were purified from OT-II transgenic mice by negative selection using antibodies to CD8a, CD11b, CD11c, CD19, CD45R, CD49b, CD105, Anti-MHC-class II, and Ter-119 according to the manufacturer's instructions. DC were pulsed with OVA (323-339) peptide overnight and then infected with AdGFP or AdIKK for 48 hours. DC were then co-cultured with OT-I CD8 T cells or OT-II CD4 T cells and proliferation was measured by ^{3}H-thymidine incorporation as previously described (111)

2.3.6. Tissue histology and luciferase imaging

For histology, lungs were removed, inflated with 10% formalin, sutured and fixed in formalin for at least 18 hours. Sutures were removed and lungs were embedded in paraffin blocks. Lung sections were examined after hematoxylin and eosin staining. Mediastinal lymph nodes were embedded in Tissue Tek OCT compound (Sakura Fintek, Torrance, CA), and stained with hematoxylin and eosin. Lymph nodes were imaged on an Aperio ScanScope XT Automated Slide

Scanner (Vista, CA). NF-κB activation in the lungs of NF-κB luciferase mice was determined as previously described (112) with changes. Ten minutes after D-luciferin was injected, mice were euthanized by CO_2 inhalation and lungs were removed for imaging. Imaging was completed within 15 minutes after tissue harvesting on a Caliper Ivis 200 (Caliper Life Sciences, Hopkinton, MA).

2.3.7. Western blotting and electrophoretic mobility shift assays (EMSA)

Protein was prepared from whole cell or cytoplasmic extracts and Western blots were performed according to standard protocols. Rabbit anti-human IKKβ was purchased from Cell Signaling Technology (Boston, MA) and anti-actin-HRP and anti-rabbit-HRP was purchased from Santa Cruz Biotechnology (Santa Cruz, CA). To detect NF-κB activity, nuclear protein was extracted and EMSA was performed. Briefly, cells were washed in PBS then suspended in CE buffer (10mM HEPES (pH7.9), 10mM KCl, 0.1mM EDTA, 0.3% NP-40, and 1x Protease inhibitors) for 5 min. at 4℃, then centrifuged for 5 min at 1600xg. The supernatant (cytoplasmic extract) was removed and the remaining pellet was washed in CE buffer without NP-40. Finally the pellet was suspended in NE buffer (20mM HEPES (pH7.9), 0.4M NaCl, 1mM EDTA, 25% glycerol) and incubated on ice for 10 minutes with intermittent vortexing. The supernatant (nuclear extract) was collected after centrifugation (16,000xg for 5 min). To detect NF-κB activity, the following hairpin oligonucleotide was used as a probe: GAGAGGGGATTCCCCGATTACCTTTCGGGGAATCCCCTCT. The probe was annealed and end-labeled with Gamma-ATP using T4 polynucleotide kinase according to the manufacturer's instructions (New England Biolabs). Labeled

probes (25,000cpm/rxn) were incubated with nuclear extracts, NF-κB Binding Buffer (50mM Tris (pH7.6), 250mM NaCl, 2.5mM EDTA, 5mM DTT, 1mg/mL BSA, 25% Glycerol) and 1ug poly-dI:dC for 20 min at room temperature and separated on a 10% non-denaturing polyacrylamide gel with 0.25X TBE running buffer. The gel was dried at 80ºC for 2 hours and then exposed to film overnight at –80ºC.

2.3.8. RNase protection assay (RPA) and qPCR

RNA was purified using Trizol® Reagent (Invitrogen, Carlsbad, CA) following the manufacturer's instructions for RPA. To detect mRNA expression of cytokines in DC, RPA probe sets hCK2b, mCK2b and mCK3b (BD Pharmingen, San Diego, CA) were used. For qPCR, RNA was purified from culture using the RNEasy kit from Qiagen (Valencia, CA) according to the manufacturer's protocol including the on-column DNase digestion. Lung tissue was homogenized in a bead beater (BioSpec, Bartlesville, OK) prior to extraction by adding 60 mg of lung tissue to 1.2 ml Buffer RLT + 2-ME (Qiagen RNEasy kit) and filling a 2.0 ml tube with 1.0 mm glass beads. Samples were subjected to 3-4 50-second homogenizations on the bead beater. RNA samples were reverse-transcribed and then subjected to quantitative PCR analysis in an Applied Biosystems 7900HT Sequence Detection System (Carlsbad, CA) with SYBR Green I Master Mix (Applied Biosystems, Carlsbad, CA) using gene-specific primers. Primer quality was validated by checking for a single dissociation curve. All samples were run in triplicate and were normalized to β-actin. Primers used for qPCR are listed in Table 2.1.

Table 2.1. *RT-PCR primer list*. Primers were used for RT-PCR in mouse lung cells and BMDC.

Gene	Forward Primer	Reverse Primer
β-actin	5'-ATGGAATCCTGTGGCATCCAT-3'	5'-CCACCAGACAACACTGTGTTGG-3'
IFNβ	5'-AGCTCCAAGAAGGACGAACAT-3'	5'-GCCCTGTAGGTGAGGTTGATCT-3'
IL-6	5'-CTGCAAGAGACTTCCATCCAGTT-3'	5'AGGGAAGGCCGTGGTTGT-3'
TNFα	5'-AGCCGATGGGTTGTACCTTGTCTA-3'	5'-TGAGATAGCAAATCGGCTGACGGT-3'
IL-12p35	5'-ACCTGCTGAAGACCACAGATGACA-3'	5'-TAGCCAGGCAACTCTCGTTCTTGT-3'
IL-12p40	5'-ATGTGGGAGCTGGAGAAAGACGTT-3'	5'-ATCTTCTTCAGGCGTGTCACAGGT-3'

2.3.9. ELISA and ELISpot assays

Peripheral blood was collected from mice at D9 and/or D21 after adenovirus administration via submandibular puncture and serum was collected. Anti-GFP IgG ELISAs were performed as previously described (68). Relative amounts of anti-GFP IgG were calculated by creating a linear regression model using two-fold serial dilutions of GFP-positive serum. The relative difference of each sample OD450 measurement was determined by best-fit curve. GFP protein was purchased from Clontech Laboratories (Mountain View, CA). Anti-mouse IgG-HRP was purchased from Jackson ImmunoResearch Laboratories (West Grove, PA). For detection of CD8 T cells secreting IFN-γ, enzyme-linked immunosorbent spot (ELISpot) assays were performed as described (113). Briefly, CD8 T cells were purified from whole splenocytes of mice by positive selection using anti-CD8 coated magnetic beads (Miltenyi Biotec, Auburn, CA). Whole draining lymph nodes from mice were mechanically disrupted and passed through a 40 μm mesh filter to produce a single cell suspension. Mouse lungs were processed as previously described (114) and the T cell enriched population was used. Responder (CD8, lymph node or enriched lung) cells were incubated at different concentrations per well, together with $1x10^5$ stimulator cells (unpulsed or peptide pulsed cells). EL4 cells were pulsed with the OVA peptide SIINFEKL for OVA-specific ELISpots and P815 cells pulsed with the GFP peptide HYLSTQSAL for GFP-specific ELISpots. Cells were cultured for 24 hours at 37ºC and spots (IFN-γ producing cells) were developed. Purified anti-mouse IFN-γ (capture) antibodies, biotinylated anti-mouse IFN-γ (detection) antibodies and

streptavidin-HRP antibodies were purchased from eBioscience (San Diego, CA). AEC detection substrate was purchased from BD Pharmingen (San Diego, CA). Spot counting was done with an AID EliSpot Reader System (Autoimmun Diagnostika GmbH, Strassberg, Germany).

2.3.10. Statistical analysis

All figures represent results from at least two independent experiments. Where appropriate, results are expressed as mean +/- SEM.

2.4. Results

2.4.1. Constitutively-active IKKβ induces maturation of DCs and induction of cytokines

IKKβ is the primary activator of NF-κB p50, RelA (p65) and cRel subunits in response to most stimuli (17, 27, 41, 102). Mutation of serines 177 and 181 to glutamic acid (IKKβEE) locks IKKβ into an active conformation and is sufficient for activation of NF-κB (44, 46) We generated a replication-deficient adenovirus type 5 that expresses IKKβEE (AdIKK) and GFP using dual CMV promoters (Fig 2.1A). HEK-293T cells infected with AdIKK showed high IKKβ expression and nuclear NF-κB translocation compared to an adenovirus that only expresses GFP (AdGFP) (Fig. 2.1B).

Dendritic cells are the main cellular link between innate and adaptive immunity (22). As such, they can play an integral part in successful vaccine-induced immunity. They have the ability to react directly to TLR stimulation and subsequently activate T cells and the adaptive immune system through direct

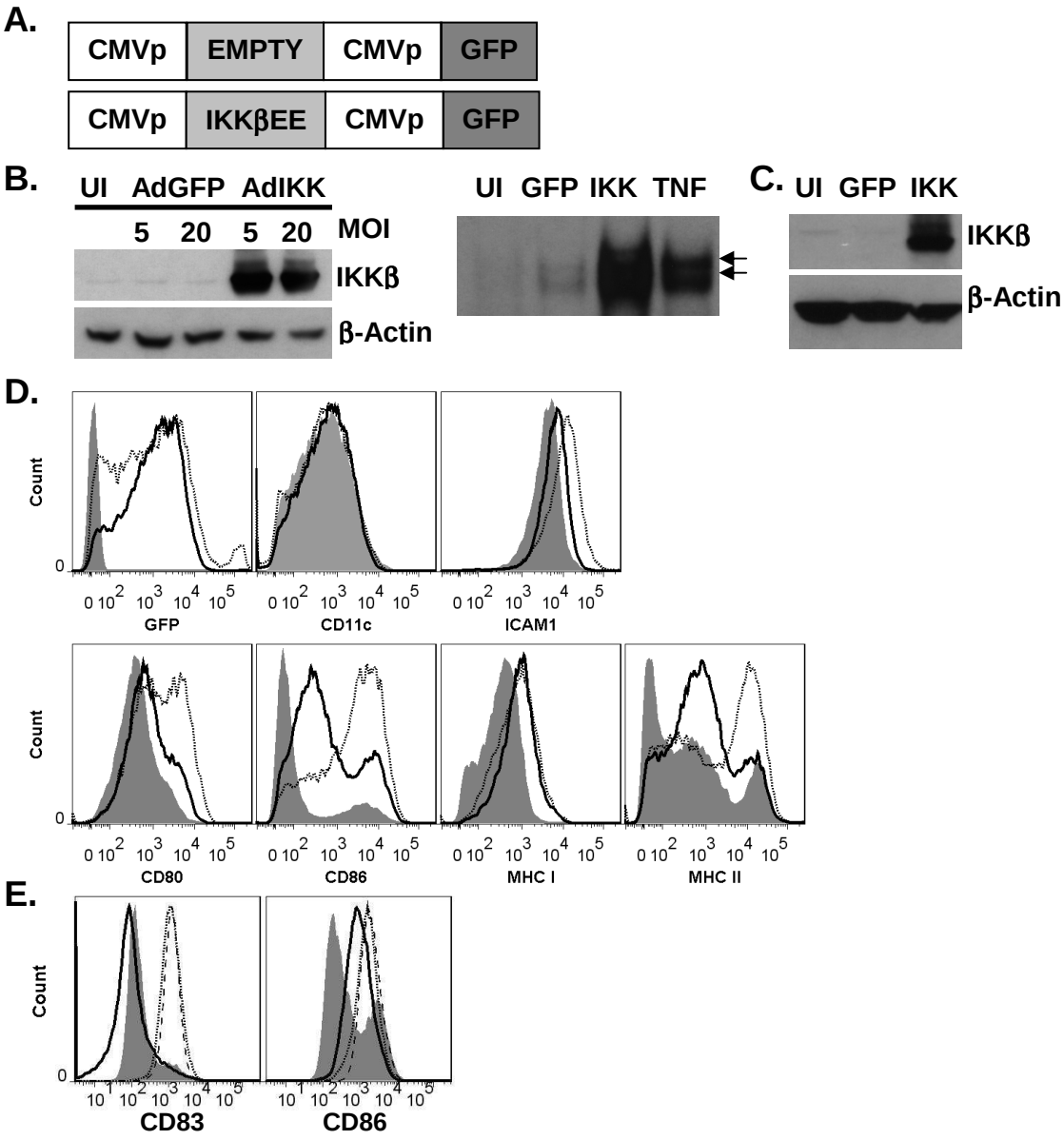

Figure 2.1. *Impact of AdIKK infection on murine and human dendritic cells.* (A) Depiction of the DUAL-GFP-CCM shuttle vector used to create AdGFP and AdIKK. (B) Western blot showing IKKβ expression in HEK-293T cells uninfected (UI) or infected with AdGFP or AdIKK (MOI=5 or 20, 48h) (left), EMSA showing nuclear expression of NF-κB in HEK-293T cells uninfected, infected with AdGFP or AdIKK (MOI=5, 48h), or treated with TNFα (20 ng/ml, 2h). (C) Western blot showing IKKβ expression in murine BMDC uninfected or infected with AdGFP or AdIKK (MOI=200, 48h). (D) FACS analysis of maturation markers on murine BMDC after infection with AdGFP or AdIKK (MOI=200, 48h). Uninfected: shaded, AdGFP: solid black line, AdIKK: dotted line. (E) FACS analysis of human MoDC after infection with AdGFP or AdIKK (MOI=500, 48h) or treatment with LPS (10 ng/ml, 16h). Uninfected: shaded, AdGFP: solid black line, AdIKK: dotted line, LPS: dashed line. Results are representative of at least two independent experiments. GFP: AdGFP. IKK: AdIKK. TNF: TNFα

interaction with cells and cytokine production. Infection of murine BM-derived DCs (BMDCs; generated as described (24)) with AdIKK induced high IKKβ within 48 hours (Fig 2.1C). Maturation of BMDC was also induced by AdIKK infection via increased expression of key T-cell stimulatory molecules CD80, CD86, MHC class II (I-A^b) and ICAM-1 shown by FACS (performed as described (24)). Importantly, both AdIKK and AdGFP led to similar levels of GFP expression following BMDC infection (Fig 2.1D). Infection of human MoDC with AdIKK also resulted in increased expression of CD83 and CD86 to levels similar to those induced by LPS stimulation (Fig 2.1E).

In contrast, AdIKK did not increase the expression of MHC class I (H2-K^b) over AdGFP infected cells (Fig 2.1D). However, AdIKK increased expression of IFN-β, IL-6 IL-12p40, IL-12p35 (Fig 2.2A) TNF-α, IL-1α and IL-1β (Figure 2.2B), and protein expression of IL-6 and IL-12 (Fig. 2.2C). Infection of human MoDC with AdIKK also resulted in increased expression of IL-12p35 and p40, IL-1a, IL-1b, IL-1RA, IL-6, and IFN-γ (Fig 2.2D). While numerous signaling pathways are known to participate in regulating DC function, these findings indicate that activation of IKKβ is sufficient for robust induction of expression of key cell surface molecules and cytokines in both mouse and human DC.

2.4.2. AdIKK induces the expression of both pro-inflammatory and T-cell stimulating cytokines through p50 and cRel

Previous work in our lab has shown that different NF-κB subunits are responsible for the induction of inflammatory cytokines and T cell-activating

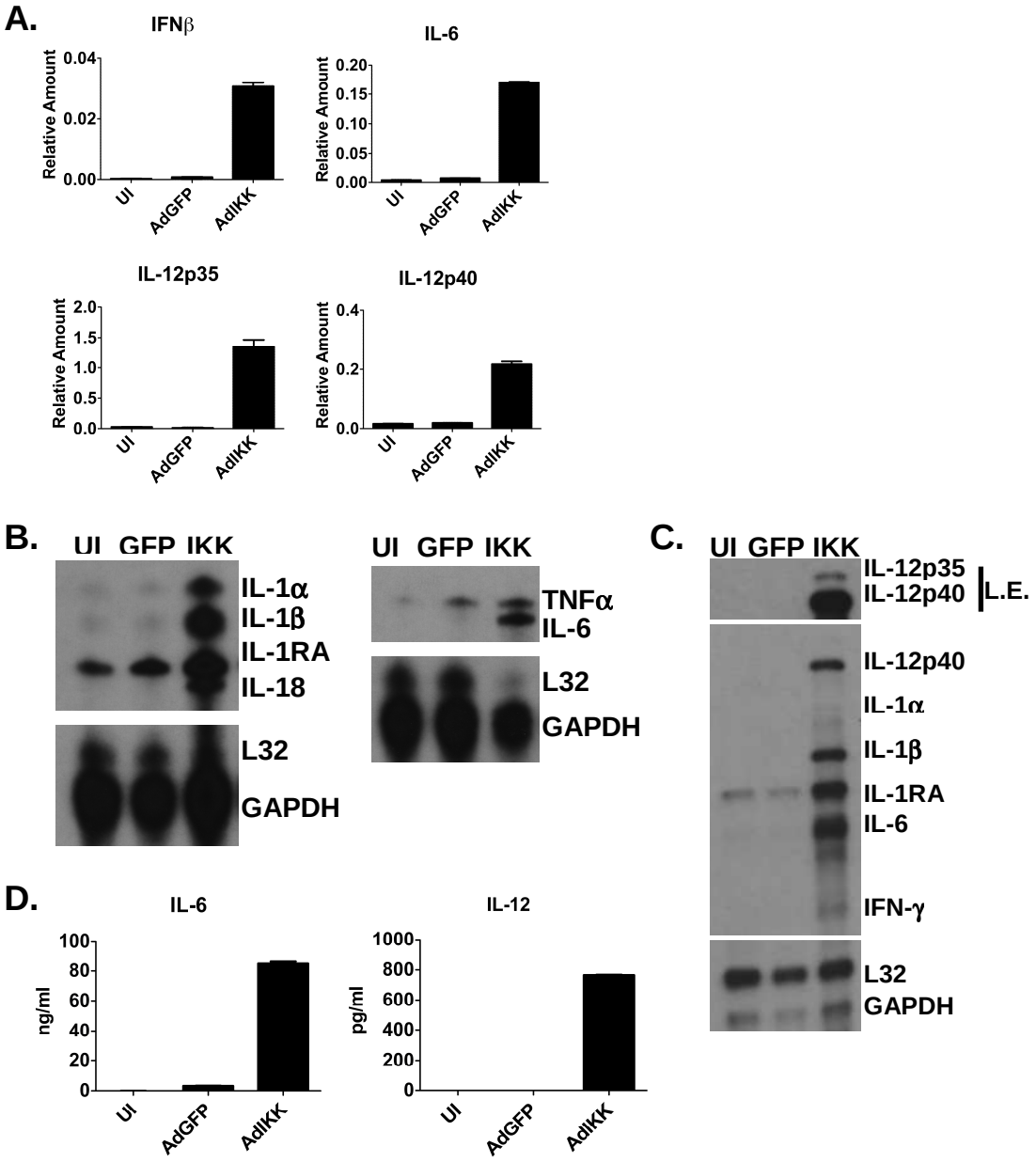

Figure 2.2. *Impact of AdIKK infection on cytokine expression in dendritic cells.* (A) RT-PCR of C57Bl/6 BMDC showing cytokine induction after infecting cells with AdGFP or AdIKK (MOI=200, 48h) or leaving cells uninfected (UI). Results are averaged from triplicate samples +/- SEM. (B) RPA of C57Bl/6 BMDC showing cytokine induction after AdGFP or AdIKK infection (MOI=200, 48h). (C) RPA of human MoDC showing cytokine induction after AdGFP or AdIKK infection (MOI=500, 48h). L.E.= long exposure. (D) ELISAs showing cytokine expression in C57Bl/6 BMDC after infection with AdGFP or AdIKK (MOI=200, 48h). Samples were run in triplicate and results are reported as average +/- SEM. Results are representative of at least two independent experiments. GFP: AdGFP. IKK: AdIKK.

cytokines in DC (24). To determine which canonical NF-κB subunits were activated by AdIKK, we examined nuclear translocation of RelA/p65, cRel and p50 in murine BMDCs after infection with AdGFP or AdIKK. Translocation of all three subunits was increased in AdIKK-infected BMDCs compared to AdGFP-infected BMDCs (Figure 2.3A). We next determined whether RelA, cRel, or p50 were required for AdIKK-induced cytokine production. To this end, we used BMDCs deficient in RelA or p50+cRel as described (24). Interestingly, unlike LPS stimulation (24), RelA was not required for the induction of IL-6 in DCs after AdIKK infection (Fig 2.3B). However, loss of p50 and cRel greatly decreased the induction of IL-6, IL-12p40 and IL-12p35 (Fig 2.3B, C). These results indicate that AdIKK infection predominantly activates cytokine expression through p50 and cRel.

2.4.3. AdIKK infected DCs are not superior stimulators of T-cell responses

We next examined the ability of AdIKK-infected BMDCs to activate $CD8^+$ T cells. BMDCs were pulsed with ovalbumin (OVA) SIINFEKL peptide as described (111) followed by infection with AdIKK or AdGFP. Surprisingly, although AdIKK increased maturation marker and inflammatory cytokine expression, BMDCs infected with AdIKK were incapable of increasing proliferation of OVA-specific OT-1 T cells compared to AdGFP-infected or uninfected BMDCs (Fig 2.4A). This is consistent with previous results showing no difference in MHC I molecule expression on BMDC. Since AdIKK infection of BMDCs increased MHC class II expression compared to AdGFP (Fig 2.1D), we also examined their ability to

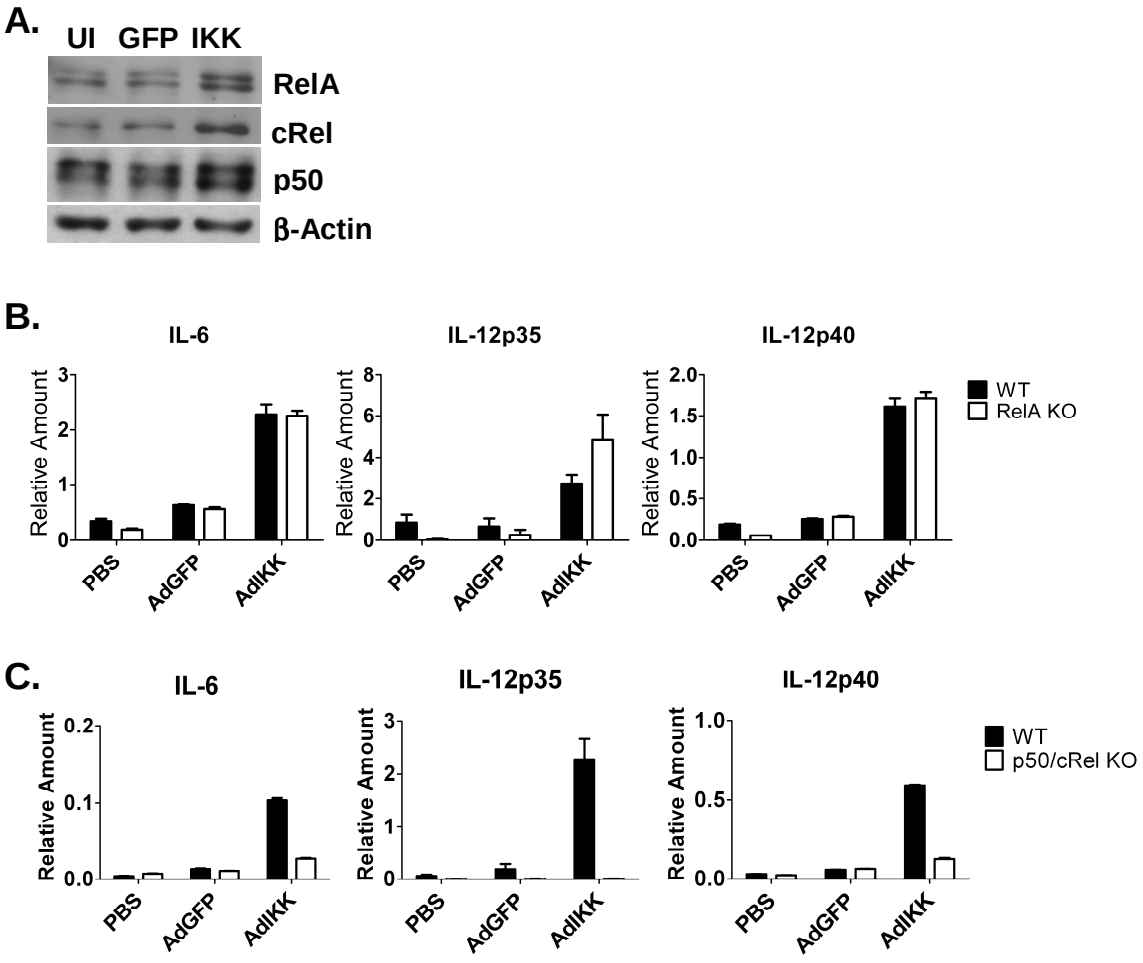

Figure 2.3. *Role of classical NF-κB subunits in AdIKK responses.* (A) BMDCs were either uninfected or infected with AdGFP or AdIKK (MOI=200, 48h). Western blot using BMDC nuclear extracts to detect canonical NF-κB subunits. (B, C) C57Bl/6 WT and (B) RelA KO BMDCs or (C) p50/cRel KO BMDCs were either uninfected or infected with AdGFP or AdIKK (MOI=200, 48h) and mRNA of the indicated cytokines was determined by RT-PCR, with the results normalized to β-actin expression levels. Results are representative of at least two independent experiments. UI: uninfected. GFP: AdGFP. IKK: AdIKK

induce proliferation of OVA-specific OT-II $CD4^+$ T cells. However, no significant difference in the proliferation of OT-II $CD4^+$ T cells in any group was noticed (Fig 2.4B). Therefore, AdIKK-infected BMDCs are incapable of enhancing T cell activation over control BMDCs.

We next examined the *in vivo* ability of AdIKK or AdGFP-infected BMDCs to activate and induce functional differentiation of $CD8^+$ T cells as determined by IFNγ production using ELISPOT (115). Previous studies have characterized the response of $CD8^+$ T cells to the H2-K^d-restricted GFP peptide HYLSTQSAL (116). BMDCs were infected with AdGFP or AdIKK and injected intravenously in mice. However, no increase in GFP-specific IFN-γ-producing $CD8^+$ T cells was seen in mice injected with AdIKK-infected BMDCs compared to mice injected with AdGFP-infected BMDCs after 14 days (Fig 2.4C). These experiments were repeated using 3- or 10-fold fewer BMDCs, which were injected subcutaneously. The subcutaneous administration also resulted in similar $CD8^+$ T cell activation at 7 or 15 days after injection (data not shown).

BMDC vaccine trials commonly use peptide pulsing to introduce antigens to the BMDC alone or in concert with virus infection (66). To this end, we used BMDC pulsed with exogenous peptide (SIINFEKL) prior to infection. Subcutaneous administration of pulsed and infected BMDC also showed no increase in OVA-specific IFN-γ-producing $CD8^+$ T cells in mice injected with AdIKK-infected BMDCs compared to those injected with AdGFP-infected BMDCs (Fig 2.4D). Therefore, despite the substantial increase in expression of co-

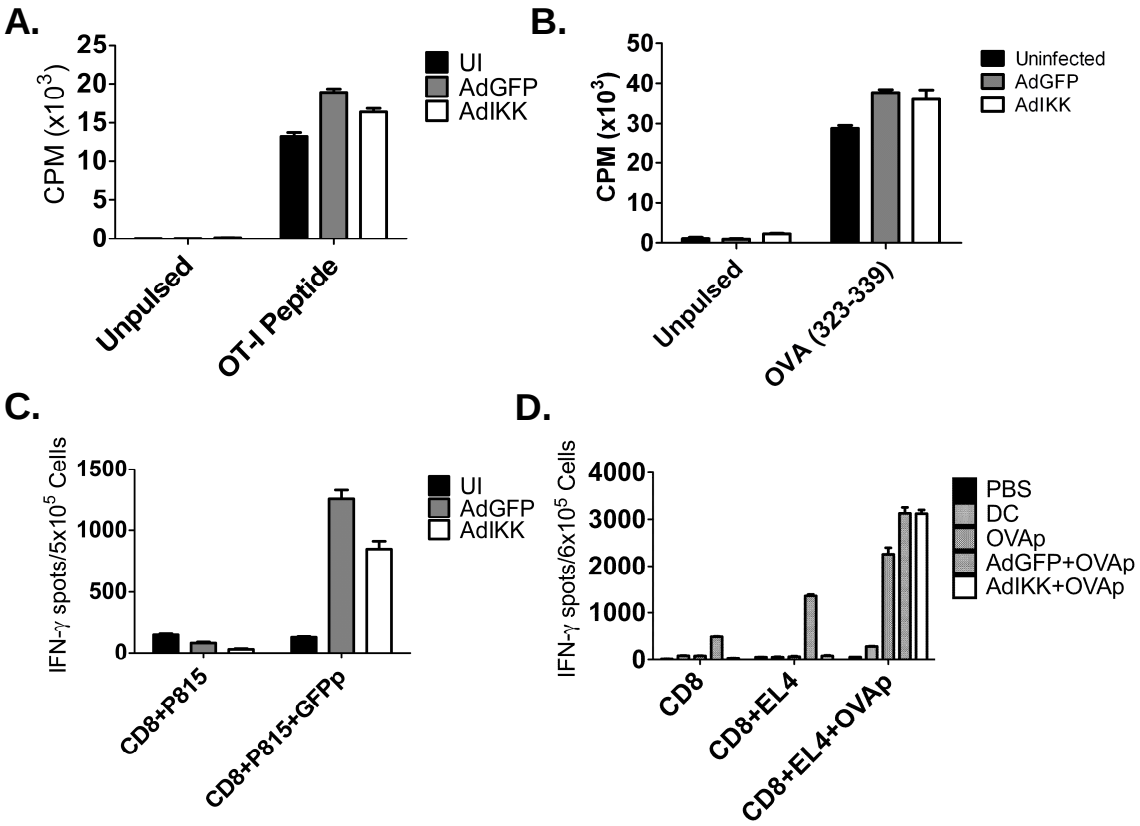

Figure 2.4. *Impact of IKK expression in BMDC on T cells.* (A) BMDCs from C57Bl/6 mice were either left untreated or pulsed with 1nM SIINFEKL overnight and then either infected with AdGFP or AdIKK (MOI=200, 48h) or left uninfected. ^{3}H-thymidine incorporation was used to measure proliferation in triplicate samples. (B) BMDC from C57Bl/6 mice were pulsed with 50nM OVA peptide (323-339) overnight and infected (MOI=250, 24h). 3H-thymidine incorporation was used to measure proliferation in triplicate samples. (C) Balb/C BMDCs were infected with AdGFP or AdIKK (MOI=500, 48h) then 1x10^{6} cells were injected intravenously into 3 Balb/C mice per group. After 14 days, CD8^{+} T cells were isolated from pooled spleens of 3 mice and IFN-γ production was determined by ELISPOT. (D) C57Bl/6 BMDCs were pulsed with SIINFEKL overnight and infected with AdGFP or AdIKK (MOI=250, 6h) then 5x10^{5} cells were injected s.c. into C57Bl/6 mice. After 6.5d, T cells were isolated from pooled splenocytes and IFN-γ production was determined by ELISPOT. Results are reported from triplicate wells as mean +/- SEM. Results are representative of at least 2 independent experiments.

stimulatory molecules and T-cell stimulating cytokines, AdIKK-infected BMDCs are not superior T cell stimulators.

2.4.4. AdIKK-induced inflammation impacts the kinetics but not the magnitude of adaptive immune response

Inflammation is known to stimulate adaptive immunity through multiple mechanisms, including APC activation, increased recruitment of leukocytes to inflammatory sites and lymphoid tissues, and direct effects on lymphocyte functions. We next determined whether potentially robust induction of pro-inflammatory cytokines by AdIKK could affect T and B cell responses. To this end, we used a pulmonary infection model that has previously been shown to induce potent inflammation (117). We first determined *in situ* NF-κB activation using a transgenic mouse strain in which NF-κB sites drive luciferase reporter gene expression (118). As shown in Fig 2.5A, AdIKK, but not AdGFP, induced strong luciferase reporter gene expression 48 hours after lung infection. The luciferase expression is most intense in the central portion of the lungs because the virus is administered intratracheally; therefore, cells near the entrance to the lungs are most likely to be infected by the virus. Inflammation was evident in the lungs of AdIKK-infected mice as early as 48 hours after administration and its effects were still present at least 21 days after administration. Lungs of mice 48 hours after AdIKK administration were markedly congested, edematous and infiltrated with numerous mixed inflammatory cells that formed prominent peri-vascular and peri-bronchiolar cuffs, and persisted for at least 21 days (Fig 2.5B).

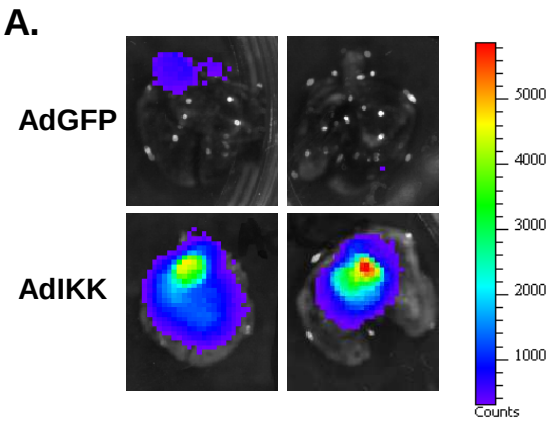
A.
AdGFP
AdIKK
5000
4000
3000
2000
1000
Counts

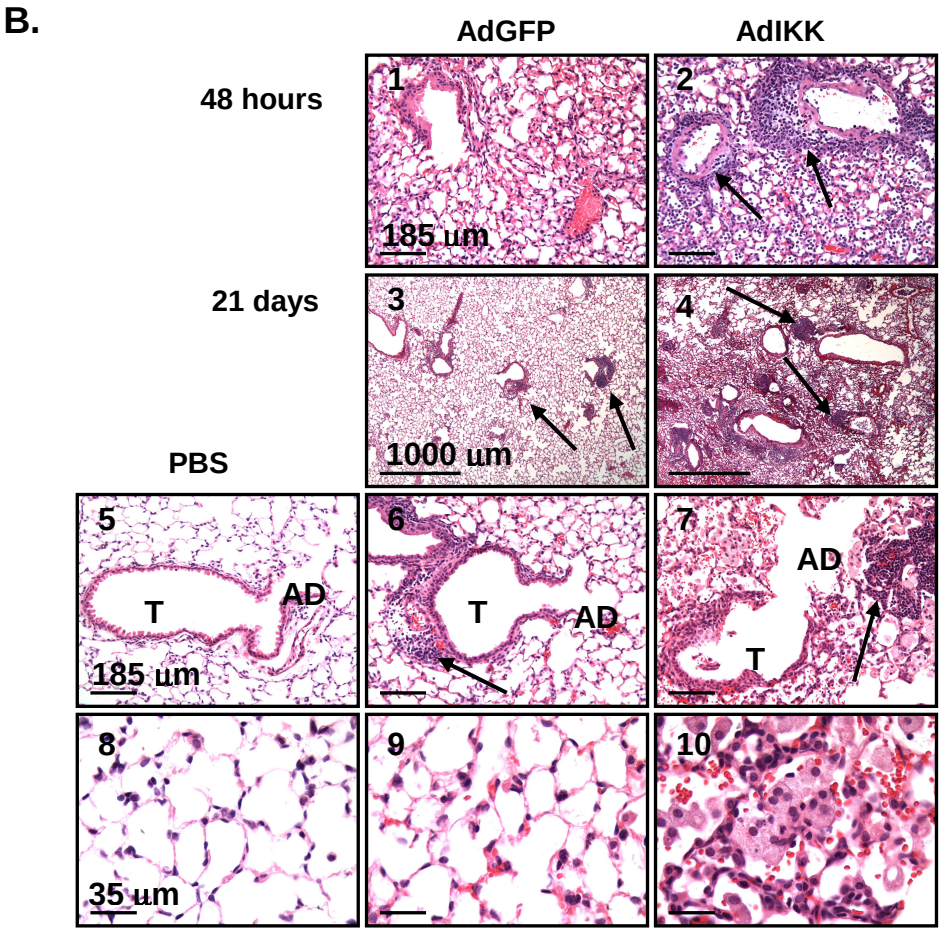
B.
AdGFP
AdIKK
48 hours
21 days
PBS
1
2
3
4
5
6
7
8
9
10
185 um
1000 um
185 um
35 um
T
AD

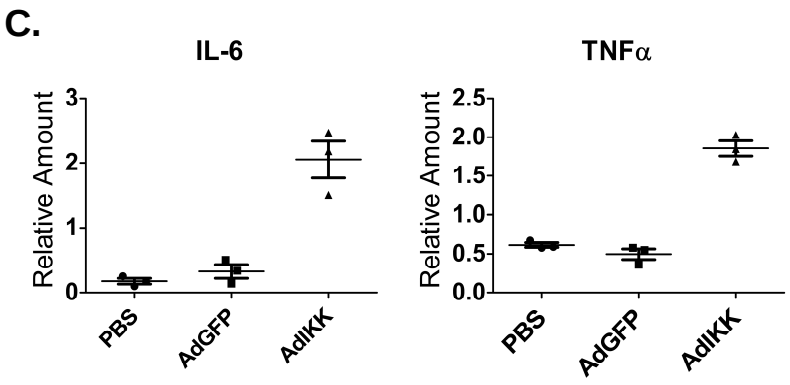

Figure 2.5. *Impact of AdIKK on the pulmonary inflammatory response.* (A) PBS or $1x10^9$ IFU AdGFP or AdIKK was administered intratracheally to NF-κB-luciferase mice. 48h after virus administration, mice were injected intraperitoneally with D-luciferin. 10 minutes later, mice were euthanized by CO_2 inhalation and lungs were removed for imaging on a Caliper IVIS 200. Imaging was completed within 15 minutes after tissue harvesting. (B) PBS or $1x10^9$ IFU AdGFP or AdIKK was administered intratracheally to C57Bl/6 mice. Lungs were removed after 48h and H&E staining was done on formalin-fixed paraffin embedded sections. Original magnification: 100x (1, 2, 5-7), 40x (3, 4), 200x (8-10). T: terminal bronchioles. AD: alveolar ducts. Scale bars for each row are the same. Arrows denote perivascular cuffing of inflammatory cells. (C) PBS or $1x10^9$ IFU AdGFP or AdIKK was administered intratracheally to 3 Balb/C mice per group followed by measurement of TNFα and IL-6 expression in total lung homogenates by RT-PCR 2 days later. Each symbol represents RT-PCR results from an individual mouse, the horizontal line represents the mean +/- SEM.

Terminal bronchioles (TB) 21 days following AdIKK-administration had undergone squamous metaplasia, and were lined by multiple layers of flattened to elongated cells with oval nuclei and slightly basophilic cytoplasm (Figure 2.5B.7), and alveolar septa (Figure 2.5B.10) were markedly thickened, hemorrhagic, infiltrated by inflammatory cells, and comprised of prominent bulging type II pneuomocytes, while alveolar sacs were filled with numerous pulmonary macrophages. In contrast, 48 hours after AdGFP administration, lungs were only mildly congested and edematous. This mild inflammation persisted for 21 days, but no other changes were evident. In agreement with the above results, RT-PCR of homogenized lungs showed a 4-fold increase in the pro-inflammatory cytokines IL-6 and TNFα after 48 hours in AdIKK-infected, but not AdGFP-infected mice (Fig 2.5C̃)

We proceeded to characterize the potential effect of NF-κB driven inflammation on the adaptive immune response to GFP as described above. While there was no substantial difference in the *percentage* of GFP-specific T cells at day 9 as determined by IFN-γ ELISPOT (not shown) the total *number* of GFP-specific T cells was substantially greater in draining LN of AdIKK-infected versus AdGFP-infected mice (Fig. 2.6A). In addition, there was a substantial increase in size and total cell numbers of draining LN of AdIKK infected mice on day 9 after infection (Fig. 2.6B). Importantly, the relative anti-GFP IgG response (determined as described (119)), on day 9 was over 3-fold higher in mice that received AdIKK compared to mice that received AdGFP (Fig 2.6C). In contrast, the total LN cell numbers, the number of GFP-specific T cells (not shown), and

A.

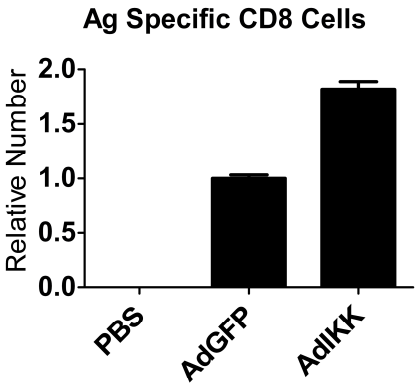
Ag Specific CD8 Cells
Relative Number
2.0
1.5
1.0
0.5
0.0
PBS
AdGFP
AdIKK

B.

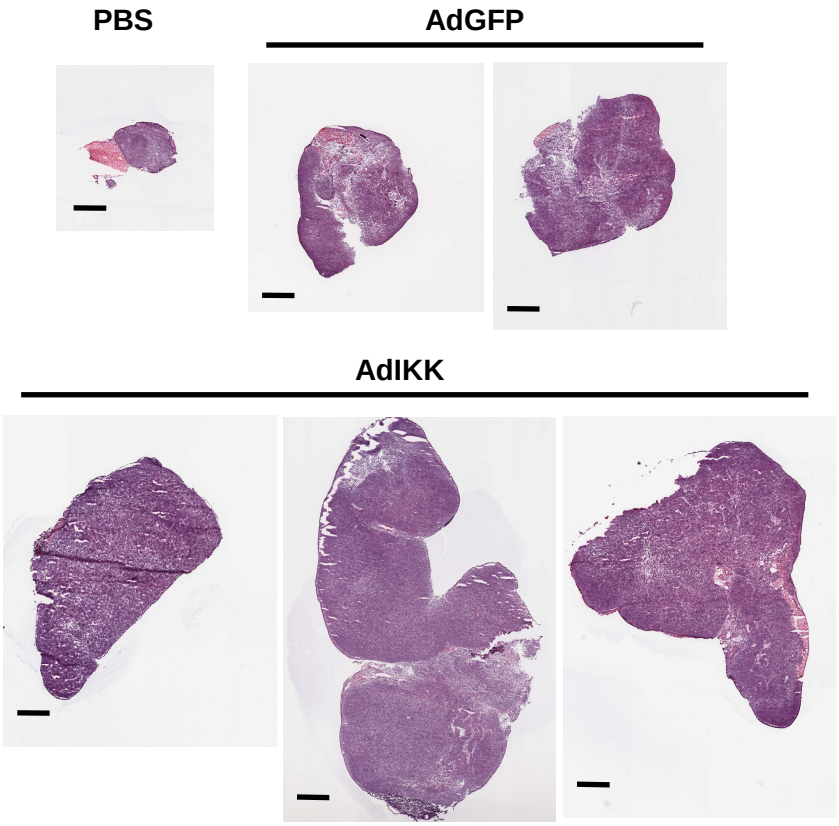
PBS
AdGFP
AdIKK

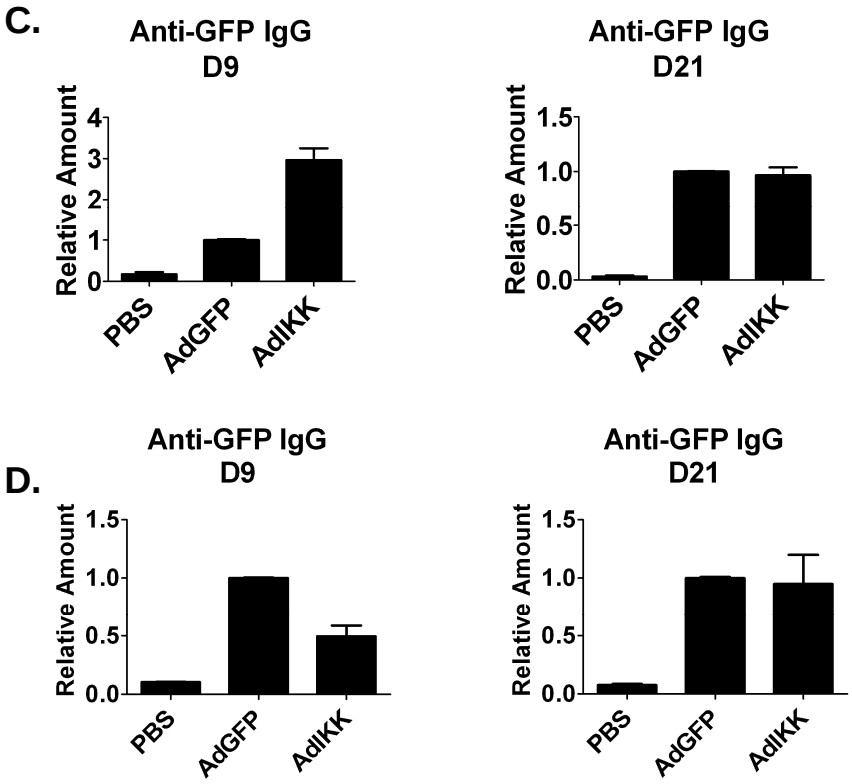

Figure 2.6. *Effect of AdIKK administration on the adaptive immune response.* (A) 10 days after intratracheal virus administration, mediastinal LNs were harvested from 3-4 mice in each of two separate experiments, pooled and total LN cells were counted. Total antigen-specific T-cell numbers were determined by ELISPOT in triplicate. The relative Ag specific $CD8^+$ T-cell numbers are from duplicate experiments plotted as fold-change compared to the AdGFP (mean and SEM). (B) PBS or $1x10^9$ IFU AdGFP or AdIKK was administered intratracheally to Balb/C mice. 9 days after administration, mediastinal lymph nodes were excised and embedded in Tissue Tek OCT. Hematoxylin and Eosin staining was performed on 5 um frozen sections and slides were imaged on an Aperio ScanScope XT Automated Slide Scanner. All images are captured at the same magnification. Scale bars represent 500 um. (C) Serum was pooled from 3 mice infected intratracheally with AdGFP or AdIKK after 9 and 21 days. The anti-GFP IgG response was measured by ELISA. Samples were read in triplicate, relative antibody levels were determined by interpolation of a dilution curve run in parallel to the samples. Results from duplicate experiments are plotted as fold-change compared to the AdGFP controls (mean and SEM). (D) Performed as in (C) except mice were injected s.c. in four locations with a total of $5x10^8$ IFU AdGFP or AdIKK. Serum was collected at days 9 and 21 and an anti-GFP IgG ELISA was performed and analyzed as in (C). Results are representative of at least two independent experiments.

anti-GFP antibody was not different at day 21 between AdGFP and AdIKK-infected mice (Fig 2.6C). Therefore, *AdIKK impacts the kinetics but not the overall magnitude of an adaptive immune response*.

The patho-physiology of lungs makes them uniquely prone to induction of robust inflammation following encounter with noxious or infectious agents. We next determined if vaccination with AdIKK through alternative routes could also impact the kinetics of an antibody response. However, subcutaneous AdIKK injection had no potentiating effect on anti-GFP IgG levels on day 9 or 21 (Fig. 2.6D) nor did it induce a visible inflammatory response. These results were also evident with a 10- and 50-fold reduction in the total virus injected (data not shown). Therefore, the impact on kinetics of the adaptive immune response appears to be evident only under conditions of robust inflammation, as seen in the lungs. In conclusion, our results indicate that IKKβ primarily functions through induction of strong pro-inflammatory signals that specifically enhance the kinetics of an immune response to a viral vector.

2.5. Discussion

Previous studies have shown that adenovirus-mediated intracellular expression of NIK can strongly enhance the magnitude of an adaptive immune response in an adenovirus vaccine setting (see below) (119). Importantly, we report here that IKKβ primarily impacts the kinetics but not the magnitude of T-cell or antibody responses. The impact on kinetics is likely the result of IKKβ-

induced cytokines such as TNFα and/or TNF family members, which are known to enhance lymphocyte trafficking to LNs (120). Increased presence of lymphocytes may therefore increase the likelihood of early activation of antigen-specific lymphocytes. Our results suggest that IKKβ may be useful as an intracellular adjuvant in airway vaccines to achieve a more rapid immune response.

NIK activation of IKKα can also lead to IRF3/7 activation (121, 122). The increased magnitude of the immune response triggered by NIK (119) may therefore be mediated through combined activation of NF-κB and IRF3/7 by IKKβ/IKKα. However, in our hands, AdNIK did not increase expression of DC maturation markers and cytokines as seen with AdIKK (Fig 2.7A, B). In addition, AdNIK poorly induced nuclear translocation of canonical and non-canonical (p52 and RelB) NF-κB subunits compared to AdIKK (Fig 2.7C). In contrast, both AdIKK and AdNIK robustly induced NF-κB subunit nuclear translocation of HEK-293T cells (Fig 2.7D). It is presently unclear why AdNIK fails to activate NF-κB in BMDCs. Nonetheless, our results suggest that the main mechanism proposed by Andreakos, et al. (119) to explain AdNIK adjuvant function in mice (i.e., robust activation of NF-κB in APC), is unlikely to fully explain its immunostimulatory effects. Loss of NIK in mice results in structural defects of secondary lymphoid structures as well as impaired CD40 signaling and class switching in B cells (123-125). It is therefore possible that NIK-induced activation of adaptive immunity is mediated by profound changes in lymphoid tissue organization

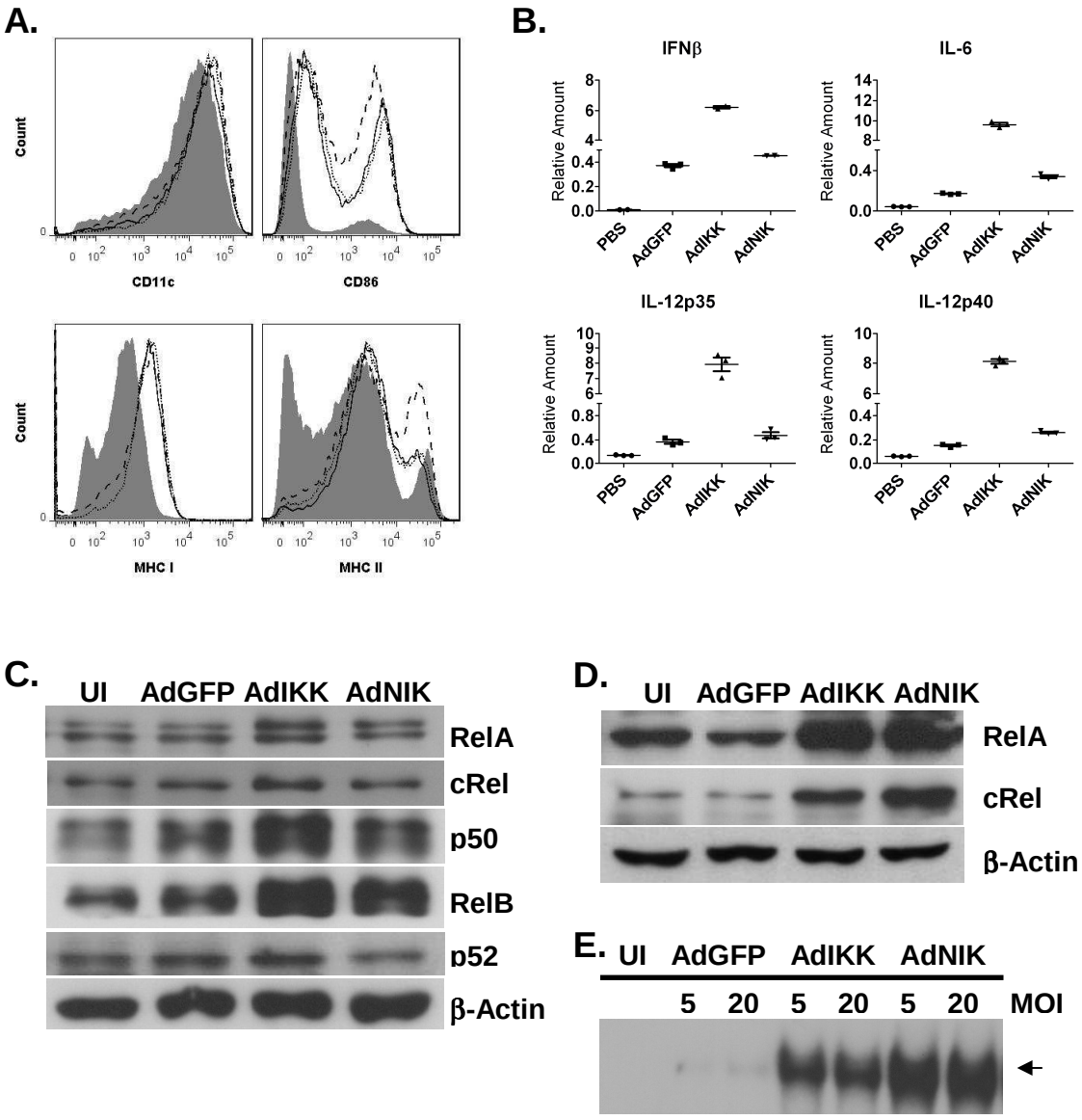

Figure 2.7. In vitro *comparison of AdIKK and AdNIK infection.* (A) Expression of co-stimulatory and maturation markers on BMDC infected with AdGFP, AdIKK, or AdNIK (MOI=200, 48h) as determined by FACS, Uninfected: shaded, AdGFP-infected: solid line, AdIKK-infected: dashed line, AdNIK-infected: dotted line. (B) Induction of cytokines in infected BMDC (MOI=200, 48h) shown by RT-PCR, results normalized to β-actin expression levels and reported as mean +/- SEM. (C, D) Western blots of nuclear extracts showing activation of NF-κB subunits in (C) BMDC (MOI 200) and (D) HEK-293T cells (MOI 20) after 48h infection. E. EMSA showing NF-κB activation in HEK293 cells after 48h infection with indicated MOI. Arrow denotes NF-κB complexes.

and/or through stimulatory effects on multiple cell types. Thus, the immunostimulatory effects of NIK and IKKβ may be mediated by distinct mechanisms. Recent studies indicate that microbial agents and inflammatory cytokines have distinct effects on DC function, with only the former promoting adaptive immunity (126). Based on our results, we suggest that microbial agent-induced activation of multiple pathways strongly promotes adaptive immunity while the exclusive activation of inflammatory cytokines/IKKβ has a more limited effect.

Major efforts are underway to understand how successful vaccines work and to define novel adjuvants that can enhance protective adaptive immunity. While virtually all microbial adjuvants activate NF-κB and IRF pathways, their specific functions in promoting adaptive immunity are not clear. Our results indicate that IKKβ canonical NF-κB pathway-induced inflammation impacts the kinetics but not the magnitude of the immune response to an adenovirus-encoded antigen. These findings therefore help define the individual role of a key pathway induced by vaccine adjuvants. A similar strategy can help determine how other major pathways, e.g., IKKα and IRF, promote adaptive immunity and whether their efficacy and underlying mechanisms are distinct from those induced by IKKβ.

Chapter 3. Crucial role of NF-κB in T cell mediated immune surveillance in murine lung cancer.

3.1. Abstract

NF-κB is constitutively activated in many tumor types and known to play a crucial role in suppressing cell death and enhancing tumor angiogenesis and metastasis. NF-κB also promotes tumor-associated inflammation characterized by neutrophil and macrophage presence, both of which promote tumor growth and invasion. Also present within the tumor microenvironment are T cells, the presence of which can be associated with immune surveillance and improved patient survival. We investigated whether in addition to known tumor promoting functions, NF-κB activation also promotes T cell mediated immune surveillance. In both primary tumors and a metastatic tumor model, we found that NF-κB expression in tumors rendered immunogenic through expression of Kb-OVA led to tumor rejection or growth suppression. Tumor growth in athymic nude mice was not affected by IKK, indicating regression was T cell mediated. IKK did not increase the overall number of T cells, nor did it make LLC-OVA cells better targets for T cells; it did increase recruitment of T cells to the tumor. Microarray results showed increases in T cell chemokines, including CCL2 and CCL5. Knock-down of CCL2 by Lentiviral shRNA in LLC-OVA-IKK cells resulted in

abrogation of tumor regression. These results suggest that NF-κB is capable of promoting immune surveillance in a subset of tumors through increased recruitment of T cells.

3.2. Introduction

A link between inflammation and cancer has been suspected since the 19th century; however, we are only beginning to understand it (89, 127). One of the main regulators of inflammation is the Nuclear Factor-κB (NF-κB) family of transcription factors (32, 48, 102). The NF-κB family consists of five members that form homodimers or heterodimers to regulate a plethora of genes. Activation of NF-κB is dependent on phosphorylation of the Inhibitors of κB (IκB) by IKKβ (classical pathway) and IKKα (alternative pathway) (17, 41, 105, 106). These two pathways are responsible for activating genes regulating varied processes, from inflammation and immunity to apoptosis (32, 37, 48, 88, 102, 128). As such, NF-κB has been shown to play a role in a number of the hallmarks of cancer (74), including self-sufficiency in growth signals, evasion of apoptosis, sustained angiogenesis, and invasion and metastasis (78, 79, 83-87). Indeed, aberrant NF-κB expression is present in many cancers including lung cancer (78), melanoma (79), multiple myeloma (80), breast cancer (81), colorectal cancer (82), and lymphoma (83).

We now know that other cells present within the tumor microenvironment play as profound a role as intrinsic tumor mutations. NF-κB expression within the tumor microenvironment can promote tumor-associated inflammation

characterized by the presence of neutrophils and macrophages, both of which promote tumor growth and invasion (77, 129). Contrary to the presence of inflammatory cells, the presence of T cells in the tumor microenvironment is associated with increased patient survival and immune surveillance (130, 131). In this study, we expressed constitutively active IKKβ in lung tumors to induce the canonical pathway and determine if NF-κB expression in tumors can promote immune surveillance.

3.3. Methods

3.3.1. Mice

Six to 8-week-old C57BL/6 mice were purchased from the National Cancer Institute (Frederick, MD). Six to 8-week-old athymic nude mice and CB6 mice were purchased from Harlan Laboratories (Indianapolis, IN). Rag 2-/- mice were kindly provided by Dr. Xue-Zhong Yu (Moffitt Cancer Center). All colonies were maintained under specific pathogen free conditions. All experiments were performed following the guidelines of the Moffitt Cancer Center and the University of South Florida Institutional Animal Care and Use Committee.

3.3.2. Cell culture

Lewis Lung Carcinoma and Turin-Bologna (TUBO) cell lines were cultured in DMEM supplemented with 10% fetal bovine serum (FBS), antibiotics, and 2mM L-glutamine. Human cells lines (H157) were cultured in RPMI supplemented with 10% fetal bovine serum (FBS), antibiotics, and 2mM L-glutamine.

3.3.3. Retroviral and lentiviral transduction

Retroviruses were prepared by transfecting HEK 293T cells with Kb-OVA, MiG or IKKβEE and packaging vectors as previously shown (24). Retrovirus transduced cells were sorted based on GFP expressing using a FACS Vantage sorter (BD Biosciences, San Jose, CA). Lentiviruses were prepared by transfecting HEK 293T cells with scrambled control pLKO.1 or pLKO.1 expressing shRNA specific for CCL2 (Open Biosystems) along with packaging vectors (24). Lentivirally transduced cells were selected for puromycin resistance.

3.3.4. Flow cytometric analysis

All transfected cell lines were tested for expression of inserted genes using FACS. MiG and IKKβ transfected lines were analyzed for GFP expression and viability. Kb OVA expressing cell lines were incubated with anti-CD16/CD32 to block Fc binding, and stained with Kb OVA-phycoerytherin for 15-20 minutes on ice. Kb-OVA expression was analyzed as well as viability. All lines showed greater than 95% GFP and/or Kb-OVA expression. Antibodies were purchased from BD Biosciences-Pharmingen (San Diego, CA). Tetramer staining was completed as described with the following changes: cells were incubated for 5 minutes at RT with Fc block and DAPI was added to cells prior to analysis for viability gating (132). p66 tetramer was kindly provided by E. Celis (Moffitt Cancer Center, Tampa, FL) and H2-Kb OVA tetramer was purchased from Beckman Coulter (Brea, CA). Flow cytometric analysis was performed on an LSR II cytometer (BD Biosciences, San Jose, CA). Aggregates and dead cells were excluded from analysis (110). Data were acquired using CellQuest software

(BD Biosciences, San Jose, CA) and analyzed using FlowJo software (Tree Star, Ashland, OR).

3.3.5. Western blotting and electrophoretic mobility shift assays (EMSA)

Protein was prepared from whole cell or cytoplasmic and nuclear extracts and Western blots were performed according to standard protocols. Rabbit anti-human IKKβ was purchased from Cell Signaling Technology (Boston, MA) and all other antibodies were purchased from Santa Cruz Biotechnology (Santa Cruz, CA). To detect NF-κB activity, EMSA was performed as described in chapter 2.

3.3.6. ELISA and ELISpot assays

Supernatant was collected from LLC-OVA-IKK cells after 48h of culture. Anti-CCL2 ELISA was performed to confirm CCL2 knockdown using the Mouse CCL2 ELISA Ready-SET-Go® kit from eBioscience (San Diego, CA) according to the manufacturer's instructions. Samples were run in triplicate.

ELISpot assays were performed as described in chapter two with the following changes: T cells were isolated from splenocytes of OT-I transgenic mice and LLC-OVA-MiG or LLC-OVA-IKK cells were used as targets.

3.3.7. Tumor studies

Cells were harvested in logarithmic growth after being cultured for less than two weeks and washed once in injection medium (phenol-free DMEM supplemented with 2% FBS) and counted. $5x10^5$ LLC cells were injected either subcutaneously (s.c.) (in a volume of 100 μl) in the right flank or intravenously (i.v.) (in a volume of 200 μl) in the tail vein. $3x10^5$ TUBO cells were injected s.c. in a volume of 100 μl. Subcutaneous tumors were monitored for growth and

measured 2-3 times per week. Mice receiving intravenous LLC injections were monitored for morbidity. Mice were sacrificed when s.c. tumors reached a diameter of 20 mm or when they showed signs of morbidity (i.v. or s.c.). Tumor volume was calculated as previously described (133).

Mice receiving TUBO cells were split into treatment and non-treatment groups on day 5, with a bias towards larger tumors in the treatment group. Immunization with p66 TriVax was performed as described on day 5 (132). The p66 peptide specific for TUBO cells was previously described (134).

3.3.8. RNA analysis

RNA was isolated using a Qiagen RNEasy kit, then reverse-transcribed and subjected to quantitative PCR analysis in an Applied Biosystems 7900HT Sequence Detection System (Carlsbad, CA) with SYBR Green I Master Mix (Applied Biosystems, Carlsbad, CA) using gene-specific primers. Primer quality was validated by checking for a single dissociation curve. All samples were run in triplicate and were normalized to β-actin.

Microarray using Mouse Genome 430 2.0 Arrays was performed on poly(A) RNA specifically converted to cDNA and then amplified and labeled with biotin using the Ambion Message Amp Premier RNA Amplification Kit (Life Technologies, Grand Island, NY) following the manufacturer's protocol (135). Hybridization with the biotin-labeled RNA, staining, and scanning of the chips followed the prescribed procedure outlined in the Affymetrix technical manual (136). Results were analyzed using Affymetrix GeneChip Operating Software

(GCOS) using the MAS 5.0 algorithm. Genes were considered changed if there was a 2-fold difference in signal compared to the control.

3.3.9. Histology

Mouse tumors were excised and sections were embedded in Tissue Tek OCT compound (Sakura Fintek, Torrance, CA) or placed in 10% formalin and subsequently embedded in paraffin blocks (FFPE). Frozen sections of mouse tumors were stained with anti-CD8 and the Rat-IgG HRP detection kit from BD Biosciences. Mouse lungs were insufflated in 10% formalin and paraffin-embedded prior to H&E staining. Lung sections were imaged on an Aperio ScanScope XT Automated Slide Scanner (Vista, CA).

3.3.10. Statistical analysis

Relative tumor growth analyzed with Fisher's Exact T test. Tetramer staining was analyzed using the Student's T test with Welch's correction.

3.4. Results

3.4.1. Critical role of IKKβ/NF-κB in T cell-induced tumor rejection

Poorly immunogenic Lewis lung carcinoma (LLC) was rendered immunogenic by expression of Kb-OVA (a single polypeptide encoding H-2K^b, β_2-microglobulin and ovalbumin SIINFEKL peptide) for recognition by CD8 T cells. Expression of IKKβ in parental (Fig 3.1A) or LLC-OVA enhanced nuclear NF-κB, comprising primarily of RelA/p65, and target gene CXCL1/KC expression (Fig 3.1B, C). However, both were substantially less than induced by TNFα (Fig 3.1B, C). Instead, NF-κB activity in LLC-OVA-IKK was comparable to a human lung

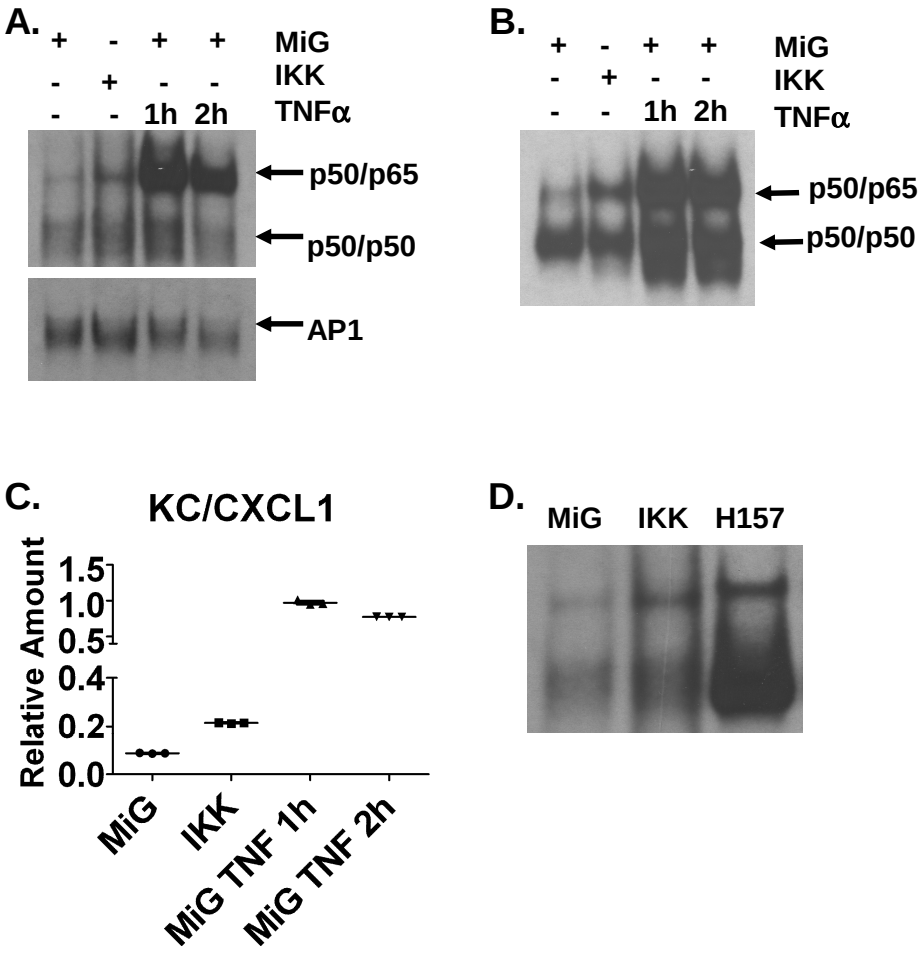

Figure 3.1. *Impact of IKKβ expression on LLC cells.* (A) EMSA showing nuclear levels of NF-κB (top) and AP1 (bottom) in LLC-MiG, LLC-IKK, or LLC-MiG cells treated with TNFα (B) EMSA showing NF-κB nuclear levels in LLC-OVA transduced with control MiG, IKK and MiG treated with TNFα for 1h and 2h as indicated. (C) RT-PCR showing KC/CXCL1 expression in LLC-OVA transduced with control MiG, IKK and MiG treated with TNFα for 1h and 2h as indicated. Samples were run in triplicate and reported as mean +/- SEM. (D) EMSA showing nuclear levels of NF-κB in LLC-OVA-MiG, LLC-OVA-IKK, or H157 cell lines. TNFα treatment: 20 ng/ml. Results are representative of at least two independent experiments.

cancer cell line harboring KRAS and p53 mutations, which are known to activate NF-κB (137) (Fig 3.1D). Compared to control LLC-MIG, LLC-IKK had no significant effect on growth of non-immunogenic LLC in syngeneic C57BL/6 mice (Fig 3.2A). In contrast, LLC-OVA-IKK tumors grew initially but were subsequently rejected (Fig 3.2B). Combined results from 3 experiments indicated that once tumors were perceptible, 10/11 LLC-OVA-MIG showed tumor growth while only 3/11 LLC-OVA-IKK showed similar growth ($p=0.004$, Fisher's Exact Test) (Fig 3.2C). Importantly, a similar number of activated OVA-specific CD8 T cells were detected in peripheral blood of mice receiving LLC-OVA-MIG and LLC-OVA-IKK (Fig 3.2D) suggesting that reduced growth of LLC-OVA-IKK was not due to impaired T cell priming. Using a metastatic LLC model, LLC-OVA-IKK showed substantially fewer and smaller lung tumor foci than LLC-OVA-MIG (or LLC-MIG and LLC-IKK) (Fig 3.2E, F). Finally, LLC-OVA-IKK grew robustly in Rag2-/- mice (Fig 3.3A) and in athymic nude mice (Fig 3.3B), demonstrating a role of lymphocytes, and more specifically, T cells, in immune rejection of LLC-OVA-IKK.

We next determined the effect of NF-κB activation in vaccine induced responses against the breast carcinoma TUBO line, which naturally express Her2/neu/p66. Five days after tumor inoculation, when tumors were perceptible, TUBO-MiG and TUBO-IKK injected mice were split into control (no vaccine) and vaccine groups. Vaccinated mice received the previously characterized Her2/Neu/p66 TriVax (132, 138) containing the p66 peptide, polyI:C as a TLR agonist, and anti-CD40. TriVax-induced responses were determined in peripheral

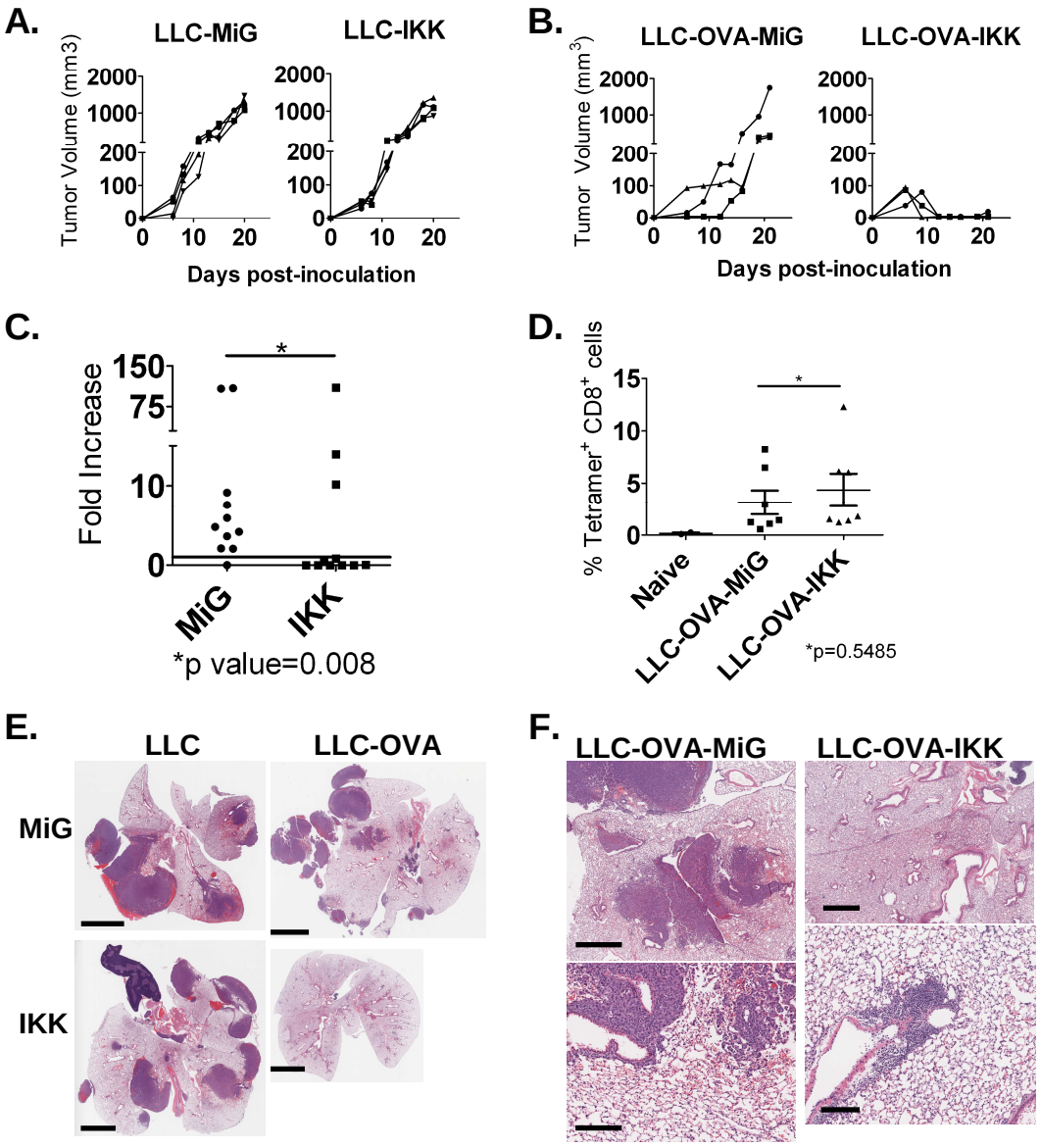

Figure 3.2. *Impact of IKKβ expression on LLC growth and T cell response in C57Bl/6 mice.* (A)Tumor growth in C57Bl/6 mice inoculated s.c. with LLC-MiG and LLC-IKK over indicated time periods. (B) Tumor growth in C57Bl/6 mice inoculated s.c. LLC-OVA-MiG and LLC-OVA-IKK over indicated time periods. Each line represents tumor growth in a single mouse. (C) C57Bl/6 mice received s.c.LLC-OVA-MiG or LLC-OVA-IKK and tumor growth was monitored. Relative fold increase in tumor volume at D21 post-inoculation compared to D4 post-inoculation. Combined results from 3 independent experiments are shown. (D) H2Kb-OVA tetramer analysis of peripheral blood on D10 from naïve mice or mice receiving LLC-OVA-MiG or LLC-OVA-IKK cells s.c. (E) H&E staining of lungs from mice 24 days after receiving *i.v.* LLC-MiG or LLC-IKK (left) or LLC-OVA-MiG or LLC-OVA-IKK. Scale bars: 4 mm (F) H&E staining of lungs from mice 24 days after receiving *i.v.* immunogenic LLC-OVA-MiG or LLC-OVA-IKK. Scale bars: 1 mm (top), and 200 μm (bottom) Results are representative of lungs from 4 mice for each condition.

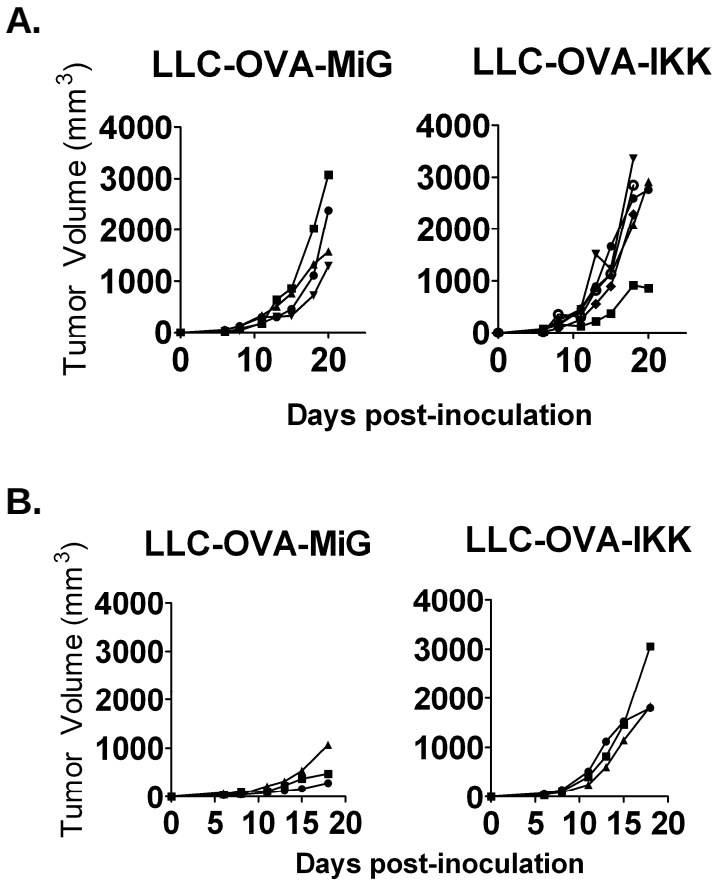

Figure 3.3. *Impact of lymphocytes on immunogenic LLC tumor growth.* (A, B) Tumor growth in (A) RAG2-/- mice or (B) athymic mice inoculated s.c. with LLC-OVA-MiG or LLC-OVA-IKK. Results are representative of two independent experiments. Each line represents tumor growth in a single mouse.

blood (Fig 3.4A). The addition of IKK had no impact on activation of p66-specific T cells. Tumor growth of vaccinated TUBO-MIG and TUBO-IKK was then determined relative to their unvaccinated counterparts. While vaccination reduced growth of both TUBO-MIG and TUBO-IKK tumors, the reduction was significantly more pronounced in TUBO-IKK ($p=0.025$) (Fig 3.4B). These results show that NF-κB activation enhances tumor rejection in spontaneous and vaccine-induced T cell priming models.

3.4.2. NF-κB induced T cell chemokine expression is crucial for tumor rejection

We next investigated potential mechanism(s) of rejection of LLC-OVA-IKK. As shown above, rejection was unlikely to be mediated by increased numbers of OVA-specific CD8 T cells (Fig 3.2D) In addition, LLC-OVA-IKK were not superior stimulators of CD8 T cell function as determined IFN-γ production (Fig 3.5A). We next examined whether NF-κB activation increases CD8 T cell recruitment in tumors. Immunohistochemistry to determine CD8 T cell presence within tumors on day 9 (i.e., prior to regression) demonstrated the presence of a small number of CD8 T cells in LLC-OVA-MIG tumors (Fig 3.5B). In striking contrast, IKK tumors showed greatly increased CD8 T cell presence as well substantial areas of tumor necrosis (Fig 3.5B). These results indicate that increased CD8 T cell recruitment may be primary reason for rejection of IKK expressing tumors.

To identify potential T cell chemokines involved, we performed microarray analysis of LLC-OVA-MIG and LLC-OVA-IKK cells. We used a 2-fold cutoff to identify genes regulated by IKKβ/NF-κB (Table 3.1). Microarray analysis identified 88 unique genes that were upregulated at least 2-fold in LLC-OVA-IKK

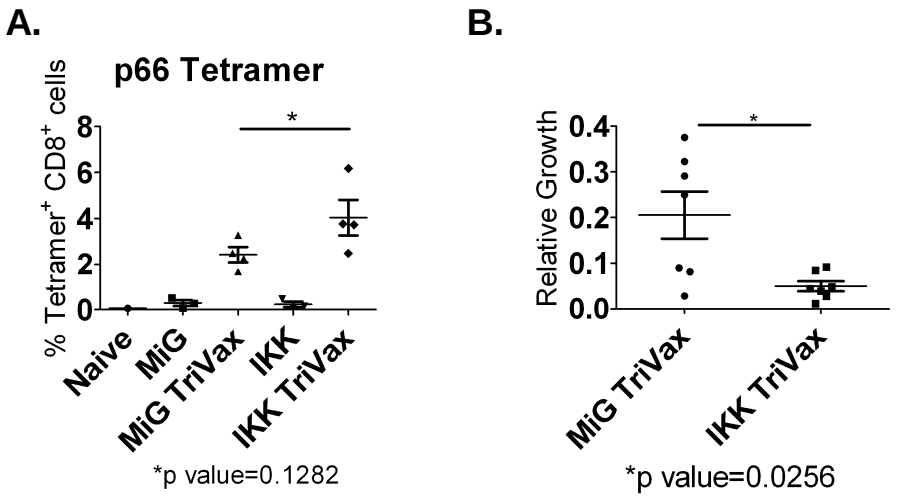

Figure 3.4. *Impact of IKKβ expression on TUBO response to p66 TriVax.*
(A) Tetramer analysis of peripheral blood on day 10 from naïve mice or mice receiving TUBO-MiG or TUBO-IKK with or without TriVax vaccination. Vaccination given on day 5. Results are representative of at least two independent experiments. P value: Student's T test with Welch's correction. (B) CB6 mice received s.c. TUBO-MiG or TUBO-IKK. After 5 days, half of the mice in each group received p66 TriVax and tumor growth was monitored. Tumor growth of all mice was calculated at D21 relative to D5 and vaccinated mice were compared relative to their unvaccinated counterparts. Results are compiled from two separate experiments. P value: Fisher's Exact Test. Results are plotted as a separate mouse for each point with mean +/- SEM.

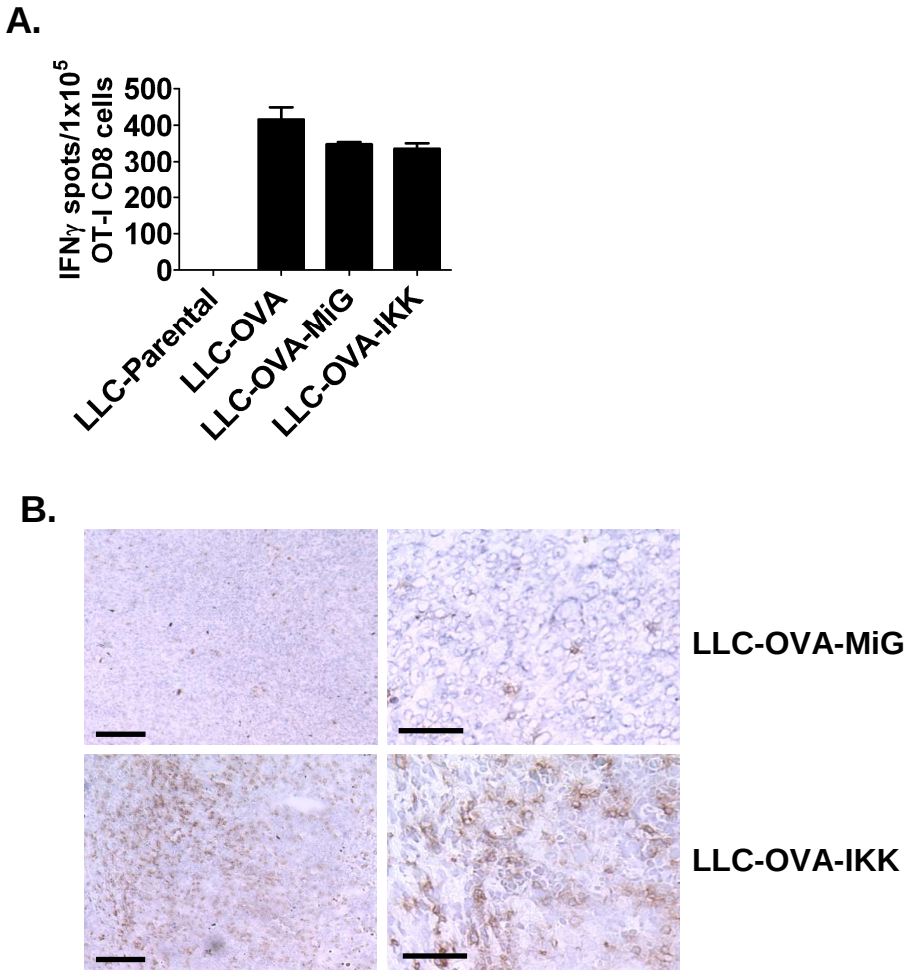

Figure 3.5. *Mechanism for T cell-induced tumor regression.* ELISpot of OT-I T cells cultured with LLC-parental, LLC-OVA, LLC-OVA-MiG, or LLC-OVA-IKK tumor cells. $1x10^5$ LLC targets/well. Samples were run in triplicate with results reported as mean +/- SEM. (B) C57Bl/6 mice received s.c. LLC-OVA-MiG or LLC-OVA-IKK. Tumors were excised at D9. Frozen sections were cut and stained for CD8 using IHC. Scale bars: 50x= 150 mm and 200x= 50 mm. Results are representative of at least two independent experiments.

Table 3.1. *Positive impact of IKKβ on genes expressed in LLC-OVA tumor cells.* Genes were identified as being increased over 2-fold in LLC-OVA-IKK cells compared to LLC-OVA-MiG cells by mircroarray. Genes are listed in order of decreasing fold-induction. Multiple probe sets for the same genes are listed and a total of 88 unique genes are upregulated in LLC-OVA-IKK cells compared to LLC-OVA-MiG cells.

Gene Symbol	Probeset	Experiment 1 Fold Change	Experiment 2 Fold Change	Average
C3	1423954_at	184.83	90.55	**137.69**
Mmp9	1448291_at	95.62	18.34	**56.98**
Casp4	1449591_at	85.50	17.08	**51.29**
Traf1	1423602_at	15.39	60.79	**38.09**
Mmp9	1416298_at	56.08	19.51	**37.80**
Tmem176a	1425603_at	14.97	28.48	**21.72**
LOC100416221	1441746_at	31.33	8.32	**19.83**
Gdpd5	1424150_at	5.39	33.77	**19.58**
Saa3	1450826_a_at	23.19	9.45	**16.32**
Pcdh1	1452294_at	26.00	6.55	**16.28**
Spt1	1448168_a_at	28.67	2.94	**15.80**
A4galt	1455338_at	22.82	7.45	**15.13**
Bcl3	1418133_at	4.11	26.11	**15.11**
Nfkbie	1458299_s_at	20.27	9.16	**14.71**
Fam84a	1425452_s_at	19.89	8.35	**14.12**
Bicd1	1437534_at	12.77	14.38	**13.57**
Cxcl10	1418930_at	11.93	14.05	**12.99**
Ccl5	1418126_at	18.09	7.72	**12.90**
4930528F23Rik	1431648_at	11.42	13.89	**12.65**
Tmem176a	1423909_at	12.19	12.23	**12.21**
Tmem176b	1418004_a_at	6.94	17.37	**12.15**
Tmem176a	1441811_x_at	9.88	14.23	**12.06**
Zfp711	1432750_at	2.43	21.60	**12.01**
Gfra2	1433716_x_at	10.93	11.62	**11.27**
Gbp2	1418240_at	18.08	3.54	**10.81**
Rbp2	1422846_at	10.15	11.18	**10.66**
H2-K1	1427746_x_at	3.21	18.03	**10.62**
Dclk1	1424270_at	17.32	2.78	**10.05**
A730089K16Rik	1437263_at	9.50	10.33	**9.92**
Stab1	1450199_a_at	12.79	5.73	**9.26**
Fabp4	1417023_a_at	6.79	11.05	**8.92**
Gpr176	1442116_at	13.98	2.37	**8.17**
Vgf	1436094_at	6.44	7.79	**7.11**
Tnfrsf9	1460469_at	9.76	4.08	**6.92**
1700049E17Rik2	1430323_at	2.71	10.58	**6.65**

Table 3.1 (continued).

Gene Symbol	Probeset	Experiment 1 Fold Change	Experiment 2 Fold Change	Average
Rrad	1422562_at	10.91	2.04	**6.48**
Nfkbie	1431843_a_at	7.86	5.00	**6.43**
Ncf4	1418465_at	4.44	8.31	**6.37**
Cd82	1416401_at	4.36	7.82	**6.09**
Ubash3a	1431698_at	3.49	8.30	**5.89**
Slc39a4	1451139_at	5.69	5.45	**5.57**
Ccl2	1420380_at	5.33	5.50	**5.42**
Ass1	1416239_at	5.90	4.86	**5.38**
Dram1	1424524_at	2.79	7.96	**5.37**
Ccdc34	1453758_at	7.29	2.88	**5.08**
Tpbpa	1415809_at	5.67	4.44	**5.05**
Slc26a3	1427547_a_at	2.79	6.90	**4.85**
Ccl7	1421228_at	5.66	4.03	**4.84**
Dclk1	1424271_at	6.79	2.83	**4.81**
Ecscr	1437451_at	5.26	4.15	**4.71**
Cxcl1	1457644_s_at	7.08	2.33	**4.71**
Arhgef3	1424250_a_at	4.06	5.18	**4.62**
Mmp13	1417256_at	5.05	4.07	**4.56**
Fas	1460251_at	6.49	2.57	**4.53**
Rnd1	1455197_at	6.00	2.49	**4.25**
Cxcl1	1419209_at	4.87	3.58	**4.22**
Ikbke	1417813_at	4.42	3.77	**4.10**
Samsn1	1421457_a_at	5.05	3.06	**4.06**
Relb	1417856_at	4.46	3.54	**4.00**
Hcn1	1450193_at	3.86	3.70	**3.78**
Nfkbia	1448306_at	4.77	2.77	**3.77**
Vegfc	1419417_at	3.48	3.77	**3.63**
LOC100044874	1424948_x_at	2.79	4.31	**3.55**
Sdk1	1440566_at	2.57	4.47	**3.52**
Trim66	1456967_at	3.35	3.34	**3.35**
Gm9855	1454180_at	2.86	3.80	**3.33**
Vegfc	1439766_x_at	3.42	3.14	**3.28**
Col8a1	1418441_at	4.50	2.04	**3.27**
Nfkbia	1449731_s_at	3.55	2.82	**3.19**
Vegfc	1440739_at	3.62	2.73	**3.18**
Pls1	1460406_at	4.26	2.01	**3.13**
Dclk1	1451289_at	4.14	2.13	**3.13**
Upp1	1448562_at	3.94	2.13	**3.03**
Slc12a8	1420334_at	3.50	2.56	**3.03**
Cxcl5	1419728_at	3.56	2.30	**2.93**

Table 3.1 (continued).

Gene Symbol	Probeset	Experiment 1 Fold Change	Experiment 2 Fold Change	Average
Col8a1	1418440_at	3.00	2.84	**2.92**
Ptpn22	1417995_at	3.13	2.69	**2.91**
Serpine2	1416666_at	2.35	3.24	**2.80**
Gfra2	1459847_x_at	3.42	2.10	**2.76**
Nlrp3	1425412_at	2.43	3.02	**2.73**
Col8a1	1455627_at	2.55	2.83	**2.69**
Cd34	1416072_at	2.65	2.73	**2.69**
Gbp2	1435906_x_at	2.32	3.01	**2.66**
Arhgdib	1426454_at	2.84	2.44	**2.64**
Slc43a2	1434308_at	2.63	2.46	**2.55**
Igfbp7	1423584_at	2.46	2.63	**2.54**
Ubxn10	1426007_a_at	2.19	2.88	**2.53**
Marcks	1415971_at	2.38	2.68	**2.53**
Ttc39c	1426223_at	2.77	2.28	**2.52**
Nfkbia	1438157_s_at	2.73	2.30	**2.52**
Casp1	1449265_at	2.35	2.53	**2.44**
Clec4e	1420330_at	2.56	2.26	**2.41**
Scin	1450276_a_at	2.60	2.22	**2.41**
Rims1	1438305_at	2.07	2.71	**2.39**
Zfpm2	1444803_at	2.38	2.38	**2.38**
C1s Gm5077	1424041_s_at	2.48	2.26	**2.37**
Mmp3	1418945_at	2.55	2.18	**2.37**
H2-K1	1425336_x_at	2.62	2.10	**2.36**
Casp12	1449297_at	2.09	2.56	**2.33**
Limd2	1447766_x_at	2.01	2.64	**2.32**
Fjx1	1422733_at	2.57	2.06	**2.32**
Cxcl1	1441855_x_at	2.11	2.52	**2.32**
Nfasc	1459113_at	2.33	2.21	**2.27**
Med8	1442417_at	2.06	2.40	**2.23**
Nfkbia	1420088_at	2.19	2.09	**2.14**
Pdgfra	1421917_at	2.19	2.07	**2.13**

cells compared to LLC-OVA-MiG cells. These included multiple chemokines involved in both T cell and neutrophil chemotaxis (Fig 3.6A, Table 3.2). Amongst T cell chemokines identified, CCL2, CCL5 and CXCL10 are known to mediate activated T cell chemotaxis (139). RT-PCR confirmed upregulation of CCL2, CCL5 (Fig 3.6B) and other chemokines (data not shown) in LLC-OVA-IKK. CCL2 in particular exhibited high net expression in LLC-OVA-IKK (Fig 3.6A). Previous studies have indicated conflicting roles for CCL2 in anti-tumor T cell responses and an important role in breast cancer metastasis (140-142). Given these diverse functions, we determined whether CCL2 was specifically required for rejection of LLC-OVA-IKK by knockdown (KD) of CCL2 expression with shRNA-expressing lentiviruses. We identified an shRNA that led to greater than 80% reduction in CCL2 protein expression by ELISA (Fig 3.6C). CCL2 KD did not impact LLC growth *in vitro* (data not shown). LLC-OVA-IKK transduced with control or CCL2 lentivirus resulted in similar expansion of OVA-specific T cells (Fig 3.6 D). However, while control LLC-OVA-IKK tumors were readily rejected, CCL2 KD resulted in robust tumor growth (Fig 3.6E). These results therefore identify CCL2 as a crucial NF-κB target gene that is required for LLC rejection.

3.5. Discussion

The tumor promoting functions of NF-κB have been extensively documented. We report here that in immunogenic tumors or following administration of anti-tumor vaccines, high NF-κB activity leads to tumor rejection and/or retardation of tumor growth.

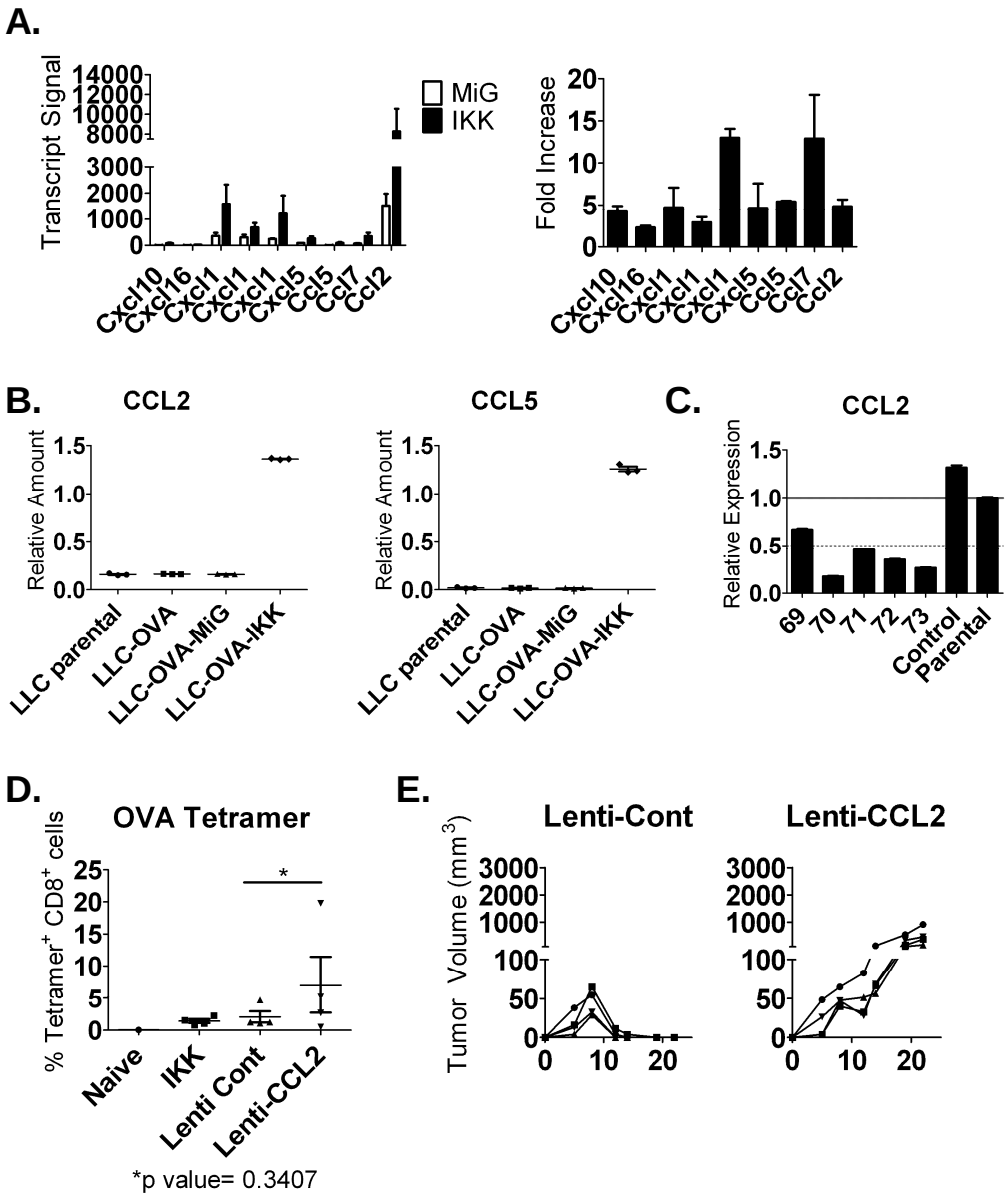

Figure 3.6. *Impact of T cell chemokines on tumor rejection.* (A)Transcript signal (left) and fold increase (right) of chemokines induced by LLC-OVA-IKK at least two-fold over LLC-OVA-MiG determined by microarray. Genes reported as mean +/- SEM. (B) Tetramer analysis of peripheral blood on D14 from naïve mice or mice receiving LLC-OVA-IKK, LLC-OVA-IKK-Lenti control or LLC-OVA-IKK-CCL2. Each point represents data from a single mouse. (C) RT-PCR showing CCL2 and CCL5 expression in LLC parental, LLC transduced with OVA and LLC transduced with OVA+MiG or OVA+IKK. Results normalized to β-actin levels. Samples were run in triplicate and reported as average +/- SEM. (E) LLC-OVA-IKK-Lenti control and LLC-OVA-IKK-CCL2 cells were injected s.c. in C57Bl/6 mice and tumor growth was monitored. Each line represents growth in a single mouse. All results are representative of at least two independent experiments.

Table 3.2. *Positive impact of IKKβ on chemokines expressed in LLC-OVA tumor cells.* Chemokines were identified as being increased over 2-fold in LLC-OVA-IKK cells compared to LLC-OVA-MiG cells by mircroarray. Genes are listed in order of decreasing fold-induction.

Gene Symbol	Probeset	Experiment 1 Fold Induction	Experiment 2 Fold Induction	Average Fold Induction
Cxcl10	1418930_at	11.93	14.05	**12.99**
Ccl5	1418126_at	18.09	7.72	**12.90**
Ccl2	1420380_at	5.33	5.50	**5.42**
Ccl7	1421228_at	5.66	4.03	**4.84**
Cxcl1	1457644_s_at	7.08	2.33	**4.71**
Cxcl1	1419209_at	4.87	3.58	**4.22**
Cxcl5	1419728_at	3.56	2.30	**2.93**
Cxcl1	1441855_x_at	2.11	2.52	**2.32**

Using tumors rendered immunogenic by antigen expression or following administration of anti-tumor vaccines, we found that high NF-κB activity leads to tumor rejection and/or growth suppression. Studies in RAG2-/- mice, which lack an adaptive immune system (143) and athymic nude mice that lack T cells (144) suggested regression was mediated in a T cell-dependent manner. Growth of LLC-OVA-MiG tumors was substantially reduced in athymic nude mice compared to RAG2-/- mice. This is most likely due to enhanced cytotoxic activity of natural killer (NK) cells present in the athymic nude mice (145).

We determined that the immunogenic tumors expressing IKK were capable of increased recruitment of T cells through increased expression of T cell chemokines, such as CCL2 and CCL5. Whether the T cells present in the tumors are specific for the expressed antigen, Kb-OVA, remains to be determined; however, that is likely the case because IKK expression in non-immunogenic LLC tumors had no effect on growth.

As mentioned above, T cell-mediated tumor regression was the result of increased chemokine expression in LLC-OVA-IKK cells. Microarray analysis of the tumor lines showed that the T cell chemokine CCL2 had the highest overall expression (although not the highest fold-induction). Knock-down of CCL2 in LLC-OVA-IKK abrogated tumor regression. Current research indicates conflicting roles for CCL2 in cancer (90, 140-142). The role of CCL2 may vary depending on its temporal and spatial expression pattern. Our model expressed CCL2 from the point of tumor ‘initiation’, and although tumors grew initially, early growth may have resulted from lower CCL2 levels. As the tumors got progressively larger,

more CCL2 was produced and the chemokine gradient increased allowing better recruitment of T cells.

CCL2 was not the only T cell chemokine induced by IKK expression, nor did it have the highest fold-induction. Other chemokines identified by our microarray data may also be playing a role in T cell-mediated tumor regression. While our results indicate a crucial role for NF-κB regulated T cell chemokines in tumor rejection, multiple additional NF-κB controlled pathways (e.g. antigen processing and presentation, expression of T cell stimulatory cytokines) may also play an important role.

Chapter 4. Concluding remarks and implications of IKKβ-induced NF-κB activation

The transcription factor NF-κB is one of the main regulators of inflammation and the immune response. NF-κB is ubiquitously expressed and is capable of activating numerous varied genes, from those involved in inhibition of apoptosis to activation of the immune response. Underscoring its central role in immunity, it is also involved in numerous diseases, from infections to autoimmunity and cancer (31, 37, 48, 102). Activation of NF-κB through the classical pathway requires functional IKKβ (42). Using constitutively active IKKβ, the studies presented here highlight two host-beneficial roles of activation of the classical NF-κB pathway.

4.1. IKKβ-induced inflammation impacts the kinetics but not the magnitude of the immune response to a viral vector

In the second chapter, we examined the role of IKKβ-induced NF-κB activation of an immune response to a viral vaccine vector. We found that IKKβ was capable of enhancing the kinetics of the immune response, but not the magnitude of the response. This impact is most likely through the induction of inflammatory cytokines, such as TNFα induced by IKKβ that are capable of

increasing lymphocyte trafficking to lymph nodes (120). Importantly, these results were only evident in cases of robust inflammation, as subcutaneous administration of AdIKK, which did not induce noticeable inflammation, was incapable of enhancing the kinetics of the immune response.

Surprisingly, while AdIKK induced increased expression of inflammatory cytokines and maturation markers in BMDCs, these increases were unable to enhance activation of T cells by the BMDCs over AdGFP infected BMDCs. Infection of BMDCs with adenovirus alone makes them capable of inducing a T cell response both *in vitro* and *in vivo* in an NF-κB-dependent manner (72). Because adenovirus already activates T cells in an NF-κB dependent manner, any further activation of DC through NF-κB may have minimal effect on T cell activation.

One additional caveat of our *in vivo* BMDC results is that the SIINFEKL OVA peptide is a very strong activator of T cells. Uninfected BMDC pulsed with SIINFEKL activated CD8 T cells to a similar level as our SIINFEKL-pulsed and AdIKK infected BMDC (Fig 2.3D). It would be interesting to examine the impact of AdIKK infection of BMDC in a less immunogenic setting, such as that of an anti-tumor immune response. Current dendritic cell based vaccines for tumor immunotherapy have fallen short of the goal of tumor eradication. This is due, at least in part, to the tolerogenic tumor microenvironment (66). In this setting, AdIKK infection of dendritic cells may be able to improve the anti-tumor immune response by overcoming tolerance. To examine this possibility, one could inject mice with tumor cells expressing known tumor associated antigens (TAA). These

mice could then be treated with DCs pulsed with the TAAs and infected with AdIKK.

In a similar study, AdNIK was shown to strongly enhance the magnitude of an adaptive immune response in an adenovirus vaccine setting (119). Here, AdNIK enhanced the type I T helper response through increased IgG2a production, T cell proliferation, IFN-γ production and cytotoxic T cells. NIK is also capable of activate IKKα and subsequent IRF family members (121, 122). This cooperative activation of NF-κB and IRF may explain the positive findings of Andreakos, et al.

In our hands, compared to AdIKK, AdNIK was unable to increase maturation markers in BMDCs, nor could it increase nuclear translocation of NF-κB family members. We did not examine the differences between the two viruses further since our AdNIK showed no difference in our preliminary studies compared to the control virus. Importantly, AdNIK was capable of increasing the expression of NF-κB target genes (IL-6, IL-12p35, and IL-12p40) in DCs at least two-fold compared to control. These results confirm that our AdNIK is functional, just not to the extent seen by Andreakos, et al. Interestingly, the predominant NF-κB subunit found in nuclear extracts from murine DCs infected with AdNIK was RelB, with some increase in p50. RelA, cRel, and p52 levels were similar to levels from AdGFP infected DCs. Infection of human HEK-293T cells with AdNIK resulted in nuclear levels of RelA and cRel similar to AdIKK-induced levels. The reasons for the differences between the two studies remain unclear; however, the majority of their *in vitro* work was completed with human DC, whereas our

comparison studies were done with murine DCs. The results from our western blots suggest that AdNIK is a more potent activator of NF-κB in human cells (our construct as well as that of Andreakos, et al uses human NIK). An additional difference between the two studies is that we used 2.5x less adenovirus to infect murine DCs, thus, any activation they saw in murine DC may be due to the higher viral titer.

Major efforts are underway to understand how successful vaccines work and to define novel adjuvants that can enhance protective adaptive immunity. While virtually all microbial adjuvants activate NF-κB and IRF pathways (4, 63), their specific functions in promoting adaptive immunity are not clear. Our results indicate that inflammation induced by IKKβ activation of the canonical NF-κB pathway impacts the kinetics but not the magnitude of the immune response to an adenovirus-encoded antigen. These findings suggest that AdIKK may be useful as an adjuvant to induce a more rapid immune response in a pulmonary disease setting. Importantly, these results help define the individual role of a key pathway induced by vaccine adjuvants.

The techniques developed in chapter 2 are now a powerful tool that can help us 1) identify the roles of other transcription factors (IKKα, NIK, IRF3) involved in the induction of adaptive immunity to adenovirus, either individually or combined, and 2) determine if activation of these pathways can act impact on our understanding of adenoviral immunity as well as the development of adenoviral vaccine vectors.

4.2. Crucial role of NF-κB in T cell mediated immune surveillance in murine lung cancer

In chapter 3, we examined the role of IKKβ-induced NF-κB in T cell mediated tumor immune responses. The role of NF-κB in tumor promotion is well documented in numerous cancer types (78, 79, 83-87). Despite the overwhelming evidence that NF-κB activation promotes cancer, we show here that IKKβ-induced activation of NF-κB can promote immune surveillance in at least a subset of tumors.

Using tumors rendered immunogenic by antigen expression or following administration of anti-tumor vaccines, we found that high NF-κB activity leads to tumor rejection and/or growth suppression. Studies in RAG2-/- mice, which lack an adaptive immune system (146) and athymic nude mice that lack T cells (144) suggested regression was mediated in a T cell-dependent manner. We determined that the immunogenic tumors expressing IKK were capable of increased recruitment of T cells through increased expression of T cell chemokines, such as CCL2 and CCL5. Whether the T cells present in the tumors are specific for the expressed antigen, Kb-OVA, remains to be determined; however, that is likely the case because IKK expression in non-immunogenic LLC tumors had no effect on growth. This question can easily be answered by using H2Kb-OVA tetramer to stain for T cells in tumors prior to regression.

As mentioned above, T cell-mediated tumor regression was the result of increased chemokine expression in LLC-OVA-IKK cells. Microarray analysis of the tumor lines showed that the T cell chemokine CCL2 had the highest overall

expression (although not the highest fold-induction). Knock-down of CCL2 in LLC-OVA-IKK abrogated tumor regression. Current research indicates conflicting roles for CCL2 in cancer (90, 140-142). The role of CCL2 may vary depending on its temporal and spatial expression pattern. Our model expressed CCL2 from the point of tumor 'initiation', and although tumors grew initially, early growth may have resulted from lower CCL2 levels. As the tumors got progressively larger, more CCL2 was produced and the chemokine gradient increased allowing better recruitment of T cells.

CCL2 was not the only T cell chemokine induced by IKK expression, nor did it have the highest fold-induction. The other chemokines identified by our microarray data may also be playing a role in T cell-mediated tumor regression. CCL2 may not be the only chemokine involved; however, loss of CCL2 is enough to abrogate tumor regression in mice. To determine if CCL2 is sufficient for tumor regression, CCL2 must be over-expressed in LLC-OVA cells. If tumors expressing CCL2 regress, it will demonstrate that CCL2 is sufficient for recruiting CD8 T cells and mediating tumor regression. If tumors do not regress, it will indicate that CCL2 induction by IKK is necessary but not sufficient for tumor regression.

The mechanisms that determine whether NF-κB functions to promote tumorigenesis or to promote anti-tumor immune responses remain to be determined. The roles of individual members of the NF-κB family, as well as the two pathways of activation need to be examined more closely. Knock-down of

individual subunits may provide a clue as to what is driving these opposing functions of NF-κB.

Clinically, NF-κB is thought of as something that should be inhibited in the treatment of cancers. Here, we have shown that activation of NF-κB can promote anti-tumor immune responses. Using constitutively active IKK is not a feasible option for the treatment of cancers due to its known role in mediating tumorigenesis and the substantial technical difficulties involved (147, 148). However, identifying tumors displaying elevated NF-κB immune surveillance functions may allow us to target them for immunotherapy. Based on our findings, we would expect greater response to immunotherapy in NF-κB high versus NF-κB low tumors.

Although NF-κB is typically associated with tumor promotion, we show here that expression of NF-κB in lung tumors can enhance the anti-tumor immune response. In mice, this surveillance is mediated by elevated chemokine expression resulting in increased T cell recruitment to the tumor.

4.3. Concluding remarks

NF-κB is involved in the activation of many genes regulating the immune response. Focusing on activation of the classical pathway of NF-κB through IKKβ, we present two stories that highlight the ability of NF-κB to enhance the immune response. In chapter 2, we show that increased activation of NF-κB in an adenoviral vaccine setting can improve the kinetics of the immune response.

In the third chapter, we show evidence supporting NF-κB activation as a mediator of increased tumor immune surveillance. These two studies provide new insights into NF-κB activation of the immune response that can be harnessed for improved treatment of diseases, including cancer.

References

1. Janeway, C. A., Jr., and R. Medzhitov. 2002. Innate immune recognition. *Annu Rev Immunol* 20:197-216.

2. Medzhitov, R. 2001. Toll-like receptors and innate immunity. *Nature reviews* 1:135-145.

3. Medzhitov, R. 2007. Recognition of microorganisms and activation of the immune response. *Nature* 449:819-826.

4. Akira, S., S. Uematsu, and O. Takeuchi. 2006. Pathogen recognition and innate immunity. *Cell* 124:783-801.

5. Kawai, T., and S. Akira. 2006. TLR signaling. *Cell death and differentiation* 13:816-825.

6. Akira, S., K. Takeda, and T. Kaisho. 2001. Toll-like receptors: critical proteins linking innate and acquired immunity. *Nature immunology* 2:675-680.

7. Yoneyama, M., M. Kikuchi, T. Natsukawa, N. Shinobu, T. Imaizumi, M. Miyagishi, K. Taira, S. Akira, and T. Fujita. 2004. The RNA helicase RIG-I has an essential function in double-stranded RNA-induced innate antiviral responses. *Nature immunology* 5:730-737.

8. Guarda, G., and A. So. 2010. Regulation of inflammasome activity. *Immunology* 130:329-336.

9. Kufer, T. A., J. H. Fritz, and D. J. Philpott. 2005. NACHT-LRR proteins (NLRs) in bacterial infection and immunity. *Trends in microbiology* 13:381-388.

10. Kato, H., S. Sato, M. Yoneyama, M. Yamamoto, S. Uematsu, K. Matsui, T. Tsujimura, K. Takeda, T. Fujita, O. Takeuchi, and S. Akira. 2005. Cell type-specific involvement of RIG-I in antiviral response. *Immunity* 23:19-28.

11. Basagoudanavar, S. H., R. J. Thapa, S. Nogusa, J. Wang, A. A. Beg, and S. Balachandran. 2011. Distinct roles for the NF-kappa B RelA subunit during antiviral innate immune responses. *Journal of virology* 85:2599-2610.

12. Kang, D. C., R. V. Gopalkrishnan, Q. Wu, E. Jankowsky, A. M. Pyle, and P. B. Fisher. 2002. mda-5: An interferon-inducible putative RNA helicase with double-stranded RNA-dependent ATPase activity and melanoma

growth-suppressive properties. *Proceedings of the National Academy of Sciences of the United States of America* 99:637-642.

13. DeVries, M. E., L. Ran, and D. J. Kelvin. 1999. On the edge: the physiological and pathophysiological role of chemokines during inflammatory and immunological responses. *Seminars in immunology* 11:95-104.

14. Bromley, S. K., T. R. Mempel, and A. D. Luster. 2008. Orchestrating the orchestrators: chemokines in control of T cell traffic. *Nature immunology* 9:970-980.

15. Li, M., D. F. Carpio, Y. Zheng, P. Bruzzo, V. Singh, F. Ouaaz, R. M. Medzhitov, and A. A. Beg. 2001. An essential role of the NF-kappa B/Toll-like receptor pathway in induction of inflammatory and tissue-repair gene expression by necrotic cells. *Journal of immunology* 166:7128-7135.

16. Richmond, A. 2002. Nf-kappa B, chemokine gene transcription and tumour growth. *Nature reviews* 2:664-674.

17. Bonizzi, G., and M. Karin. 2004. The two NF-kappaB activation pathways and their role in innate and adaptive immunity. *Trends Immunol* 25:280-288.

18. Moretta, A., E. Marcenaro, S. Parolini, G. Ferlazzo, and L. Moretta. 2008. NK cells at the interface between innate and adaptive immunity. *Cell death and differentiation* 15:226-233.

19. Banchereau, J., and R. M. Steinman. 1998. Dendritic cells and the control of immunity. *Nature* 392:245-252.

20. Banchereau, J., F. Briere, C. Caux, J. Davoust, S. Lebecque, Y. J. Liu, B. Pulendran, and K. Palucka. 2000. Immunobiology of dendritic cells. *Annu Rev Immunol* 18:767-811.

21. Shortman, K., and C. Caux. 1997. Dendritic cell development: multiple pathways to nature's adjuvants. *Stem Cells* 15:409-419.

22. Steinman, R. M., and H. Hemmi. 2006. Dendritic cells: translating innate to adaptive immunity. *Current topics in microbiology and immunology* 311:17-58.

23. Steinman, R. M., D. Hawiger, and M. C. Nussenzweig. 2003. Tolerogenic dendritic cells. *Annu Rev Immunol* 21:685-711.

24. Wang, J., X. Wang, S. Hussain, Y. Zheng, S. Sanjabi, F. Ouaaz, and A. A. Beg. 2007. Distinct roles of different NF-kappa B subunits in regulating

inflammatory and T cell stimulatory gene expression in dendritic cells. *J Immunol* 178:6777-6788.

25. Sen, R., and D. Baltimore. 1986. Multiple nuclear factors interact with the immunoglobulin enhancers. *Cell* 46:705-716.

26. Ghosh, S., and M. S. Hayden. 2008. New regulators of NF-kappaB in inflammation. *Nature reviews* 8:837-848.

27. Hayden, M. S., and S. Ghosh. 2008. Shared principles in NF-kappaB signaling. *Cell* 132:344-362.

28. Baldwin, A. S. 2001. Control of oncogenesis and cancer therapy resistance by the transcription factor NF-kappaB. *The Journal of clinical investigation* 107:241-246.

29. Baldwin, A. S., Jr. 2001. Series introduction: the transcription factor NF-kappaB and human disease. *The Journal of clinical investigation* 107:3-6.

30. Perkins, N. D., and T. D. Gilmore. 2006. Good cop, bad cop: the different faces of NF-kappaB. *Cell death and differentiation* 13:759-772.

31. Karin, M. 2006. Nuclear factor-kappaB in cancer development and progression. *Nature* 441:431-436.

32. Gilmore, T. D. 2006. Introduction to NF-kappaB: players, pathways, perspectives. *Oncogene* 25:6680-6684.

33. Beg, A. A., W. C. Sha, R. T. Bronson, S. Ghosh, and D. Baltimore. 1995. Embryonic lethality and liver degeneration in mice lacking the RelA component of NF-kappa B. *Nature* 376:167-170.

34. Burkly, L., C. Hession, L. Ogata, C. Reilly, L. A. Marconi, D. Olson, R. Tizard, R. Cate, and D. Lo. 1995. Expression of relB is required for the development of thymic medulla and dendritic cells. *Nature* 373:531-536.

35. Kontgen, F., R. J. Grumont, A. Strasser, D. Metcalf, R. Li, D. Tarlinton, and S. Gerondakis. 1995. Mice lacking the c-rel proto-oncogene exhibit defects in lymphocyte proliferation, humoral immunity, and interleukin-2 expression. *Genes Dev* 9:1965-1977.

36. Grigoriadis, G., Y. Zhan, R. J. Grumont, D. Metcalf, E. Handman, C. Cheers, and S. Gerondakis. 1996. The Rel subunit of NF-kappaB-like transcription factors is a positive and negative regulator of macrophage gene expression: distinct roles for Rel in different macrophage populations. *The EMBO journal* 15:7099-7107.

37. Ghosh, S., M. J. May, and E. B. Kopp. 1998. NF-kappa B and Rel proteins: evolutionarily conserved mediators of immune responses. *Annu Rev Immunol* 16:225-260.

38. Beg, A. A., S. M. Ruben, R. I. Scheinman, S. Haskill, C. A. Rosen, and A. S. Baldwin, Jr. 1992. I kappa B interacts with the nuclear localization sequences of the subunits of NF-kappa B: a mechanism for cytoplasmic retention. *Genes & development* 6:1899-1913.

39. Huxford, T., D. B. Huang, S. Malek, and G. Ghosh. 1998. The crystal structure of the IkappaBalpha/NF-kappaB complex reveals mechanisms of NF-kappaB inactivation. *Cell* 95:759-770.

40. Malek, S., T. Huxford, and G. Ghosh. 1998. Ikappa Balpha functions through direct contacts with the nuclear localization signals and the DNA binding sequences of NF-kappaB. *The Journal of biological chemistry* 273:25427-25435.

41. Vallabhapurapu, S., and M. Karin. 2009. Regulation and function of NF-kappaB transcription factors in the immune system. *Annu Rev Immunol* 27:693-733.

42. Hacker, H., and M. Karin. 2006. Regulation and function of IKK and IKK-related kinases. *Sci STKE* 2006:re13.

43. Hayden, M. S., and S. Ghosh. 2004. Signaling to NF-kappaB. *Genes Dev* 18:2195-2224.

44. Mercurio, F., H. Zhu, B. W. Murray, A. Shevchenko, B. L. Bennett, J. Li, D. B. Young, M. Barbosa, M. Mann, A. Manning, and A. Rao. 1997. IKK-1 and IKK-2: cytokine-activated IkappaB kinases essential for NF- kappaB activation. *Science (New York, N.Y* 278:860-866.

45. Zandi, E., D. M. Rothwarf, M. Delhase, M. Hayakawa, and M. Karin. 1997. The IkappaB kinase complex (IKK) contains two kinase subunits, IKKalpha and IKKbeta, necessary for IkappaB phosphorylation and NF-kappaB activation. *Cell* 91:243-252.

46. Delhase, M., M. Hayakawa, Y. Chen, and M. Karin. 1999. Positive and negative regulation of IkappaB kinase activity through IKKbeta subunit phosphorylation. *Science (New York, N.Y* 284:309-313.

47. Schmid, J. A., and A. Birbach. 2008. IkappaB kinase beta (IKKbeta/IKK2/IKBKB)--a key molecule in signaling to the transcription factor NF-kappaB. *Cytokine Growth Factor Rev* 19:157-165.

48. Li, Q., and I. M. Verma. 2002. NF-kappaB regulation in the immune system. *Nature reviews* 2:725-734.

49. Smith, C., E. Andreakos, J. B. Crawley, F. M. Brennan, M. Feldmann, and B. M. Foxwell. 2001. NF-kappaB-inducing kinase is dispensable for activation of NF-kappaB in inflammatory settings but essential for lymphotoxin beta receptor activation of NF-kappaB in primary human fibroblasts. *Journal of immunology* 167:5895-5903.

50. Dejardin, E., N. M. Droin, M. Delhase, E. Haas, Y. Cao, C. Makris, Z. W. Li, M. Karin, C. F. Ware, and D. R. Green. 2002. The lymphotoxin-beta receptor induces different patterns of gene expression via two NF-kappaB pathways. *Immunity* 17:525-535.

51. Yin, L., L. Wu, H. Wesche, C. D. Arthur, J. M. White, D. V. Goeddel, and R. D. Schreiber. 2001. Defective lymphotoxin-beta receptor-induced NF-kappaB transcriptional activity in NIK-deficient mice. *Science (New York, N.Y* 291:2162-2165.

52. Coope, H. J., P. G. Atkinson, B. Huhse, M. Belich, J. Janzen, M. J. Holman, G. G. Klaus, L. H. Johnston, and S. C. Ley. 2002. CD40 regulates the processing of NF-kappaB2 p100 to p52. *The EMBO journal* 21:5375-5385.

53. Claudio, E., K. Brown, S. Park, H. Wang, and U. Siebenlist. 2002. BAFF-induced NEMO-independent processing of NF-kappa B2 in maturing B cells. *Nature immunology* 3:958-965.

54. Xiao, G., E. W. Harhaj, and S. C. Sun. 2001. NF-kappaB-inducing kinase regulates the processing of NF-kappaB2 p100. *Molecular cell* 7:401-409.

55. Senftleben, U., Y. Cao, G. Xiao, F. R. Greten, G. Krahn, G. Bonizzi, Y. Chen, Y. Hu, A. Fong, S. C. Sun, and M. Karin. 2001. Activation by IKKalpha of a second, evolutionary conserved, NF-kappa B signaling pathway. *Science (New York, N.Y* 293:1495-1499.

56. van de Pavert, S. A., and R. E. Mebius. New insights into the development of lymphoid tissues. *Nature reviews* 10:664-674.

57. Hayden, M. S., and S. Ghosh. 2011. NF-kappaB in immunobiology. *Cell research* 21:223-244.

58. Chen, Z. J., L. Parent, and T. Maniatis. 1996. Site-specific phosphorylation of IkappaBalpha by a novel ubiquitination-dependent protein kinase activity. *Cell* 84:853-862.

59. Xu, G., Y. C. Lo, Q. Li, G. Napolitano, X. Wu, X. Jiang, M. Dreano, M. Karin, and H. Wu. 2011. Crystal structure of inhibitor of kappaB kinase beta. *Nature* 472:325-330.

60. Osorio, F., and E. S. C. Reis. 2011. Myeloid C-type Lectin Receptors in Pathogen Recognition and Host Defense. *Immunity* 34:651-664.

61. Beutler, B., C. Eidenschenk, K. Crozat, J. L. Imler, O. Takeuchi, J. A. Hoffmann, and S. Akira. 2007. Genetic analysis of resistance to viral infection. *Nature reviews* 7:753-766.

62. Akira, S., and K. Takeda. 2004. Toll-like receptor signalling. *Nature reviews* 4:499-511.

63. Coffman, R. L., A. Sher, and R. A. Seder. 2010. Vaccine adjuvants: putting innate immunity to work. *Immunity* 33:492-503.

64. Gautier, G., M. Humbert, F. Deauvieau, M. Scuiller, J. Hiscott, E. E. Bates, G. Trinchieri, C. Caux, and P. Garrone. 2005. A type I interferon autocrine-paracrine loop is involved in Toll-like receptor-induced interleukin-12p70 secretion by dendritic cells. *The Journal of experimental medicine* 201:1435-1446.

65. Palucka, K., H. Ueno, and J. Banchereau. 2011. Recent developments in cancer vaccines. *J Immunol* 186:1325-1331.

66. Antonia, S., J. J. Mule, and J. S. Weber. 2004. Current developments of immunotherapy in the clinic. *Current opinion in immunology* 16:130-136.

67. Liu, M. A. 2010. Immunologic basis of vaccine vectors. *Immunity* 33:504-515.

68. Cheng, C., J. G. Gall, W. P. Kong, R. L. Sheets, P. L. Gomez, C. R. King, and G. J. Nabel. 2007. Mechanism of ad5 vaccine immunity and toxicity: fiber shaft targeting of dendritic cells. *PLoS pathogens* 3:e25.

69. Tucker, S. N., D. W. Tingley, and C. D. Scallan. 2008. Oral adenoviral-based vaccines: historical perspective and future opportunity. *Expert review of vaccines* 7:25-31.

70. Bradac, J., and C. W. Dieffenbach. 2009. HIV vaccine development: Lessons from the past, informing the future. *IDrugs : the investigational drugs journal* 12:435-439.

71. Kirk, C. J., and J. J. Mule. 2000. Gene-modified dendritic cells for use in tumor vaccines. *Human gene therapy* 11:797-806.

72. Morelli, A. E., A. T. Larregina, R. W. Ganster, A. F. Zahorchak, J. M. Plowey, T. Takayama, A. J. Logar, P. D. Robbins, L. D. Falo, and A. W. Thomson. 2000. Recombinant adenovirus induces maturation of dendritic cells via an NF-kappaB-dependent pathway. *Journal of virology* 74:9617-9628.

73. Hensley, S. E., W. Giles-Davis, K. C. McCoy, W. Weninger, and H. C. Ertl. 2005. Dendritic cell maturation, but not CD8+ T cell induction, is dependent on type I IFN signaling during vaccination with adenovirus vectors. *J Immunol* 175:6032-6041.

74. Hanahan, D., and R. A. Weinberg. 2000. The hallmarks of cancer. *Cell* 100:57-70.

75. Colotta, F., P. Allavena, A. Sica, C. Garlanda, and A. Mantovani. 2009. Cancer-related inflammation, the seventh hallmark of cancer: links to genetic instability. *Carcinogenesis* 30:1073-1081.

76. Cavallo, F., C. De Giovanni, P. Nanni, G. Forni, and P. L. Lollini. 2011: the immune hallmarks of cancer. *Cancer Immunol Immunother* 60:319-326.

77. Mantovani, A., P. Allavena, A. Sica, and F. Balkwill. 2008. Cancer-related inflammation. *Nature* 454:436-444.

78. Tew, G. W., E. L. Lorimer, T. J. Berg, H. Zhi, R. Li, and C. L. Williams. 2008. SmgGDS regulates cell proliferation, migration, and NF-kappaB transcriptional activity in non-small cell lung carcinoma. *The Journal of biological chemistry* 283:963-976.

79. Yang, J., W. H. Pan, G. A. Clawson, and A. Richmond. 2007. Systemic targeting inhibitor of kappaB kinase inhibits melanoma tumor growth. *Cancer research* 67:3127-3134.

80. Annunziata, C. M., R. E. Davis, Y. Demchenko, W. Bellamy, A. Gabrea, F. Zhan, G. Lenz, I. Hanamura, G. Wright, W. Xiao, S. Dave, E. M. Hurt, B. Tan, H. Zhao, O. Stephens, M. Santra, D. R. Williams, L. Dang, B. Barlogie, J. D. Shaughnessy, Jr., W. M. Kuehl, and L. M. Staudt. 2007. Frequent engagement of the classical and alternative NF-kappaB pathways by diverse genetic abnormalities in multiple myeloma. *Cancer cell* 12:115-130.

81. Chua, H. L., P. Bhat-Nakshatri, S. E. Clare, A. Morimiya, S. Badve, and H. Nakshatri. 2007. NF-kappaB represses E-cadherin expression and enhances epithelial to mesenchymal transition of mammary epithelial cells: potential involvement of ZEB-1 and ZEB-2. *Oncogene* 26:711-724.

82. Scartozzi, M., I. Bearzi, C. Pierantoni, A. Mandolesi, F. Loupakis, A. Zaniboni, V. Catalano, A. Quadri, F. Zorzi, R. Berardi, T. Biscotti, R. Labianca, A. Falcone, and S. Cascinu. 2007. Nuclear factor-kB tumor expression predicts response and survival in irinotecan-refractory metastatic colorectal cancer treated with cetuximab-irinotecan therapy. *J Clin Oncol* 25:3930-3935.

83. Zou, P., J. Kawada, L. Pesnicak, and J. I. Cohen. 2007. Bortezomib induces apoptosis of Epstein-Barr virus (EBV)-transformed B cells and prolongs survival of mice inoculated with EBV-transformed B cells. *Journal of virology* 81:10029-10036.

84. Fernandez-Majada, V., C. Aguilera, A. Villanueva, F. Vilardell, A. Robert-Moreno, A. Aytes, F. X. Real, G. Capella, M. W. Mayo, L. Espinosa, and A. Bigas. 2007. Nuclear IKK activity leads to dysregulated notch-dependent gene expression in colorectal cancer. *Proceedings of the National Academy of Sciences of the United States of America* 104:276-281.

85. Jourdan, M., J. Moreaux, J. D. Vos, D. Hose, K. Mahtouk, M. Abouladze, N. Robert, M. Baudard, T. Reme, A. Romanelli, H. Goldschmidt, J. F. Rossi, M. Dreano, and B. Klein. 2007. Targeting NF-kappaB pathway with an IKK2 inhibitor induces inhibition of multiple myeloma cell growth. *British journal of haematology* 138:160-168.

86. Pahl, H. L. 1999. Activators and target genes of Rel/NF-kappaB transcription factors. *Oncogene* 18:6853-6866.

87. Rahman, K. M., S. Ali, A. Aboukameel, S. H. Sarkar, Z. Wang, P. A. Philip, W. A. Sakr, and A. Raz. 2007. Inactivation of NF-kappaB by 3,3'-diindolylmethane contributes to increased apoptosis induced by chemotherapeutic agent in breast cancer cells. *Molecular cancer therapeutics* 6:2757-2765.

88. Van Antwerp, D. J., S. J. Martin, T. Kafri, D. R. Green, and I. M. Verma. 1996. Suppression of TNF-alpha-induced apoptosis by NF-kappaB. *Science (New York, N.Y* 274:787-789.

89. Balkwill, F., and A. Mantovani. 2001. Inflammation and cancer: back to Virchow? *Lancet* 357:539-545.

90. Danese, S., and A. Mantovani. 2009. Inflammatory bowel disease and intestinal cancer: a paradigm of the Yin-Yang interplay between inflammation and cancer. *Oncogene* 29:3313-3323.

91. Haybaeck, J., N. Zeller, M. J. Wolf, A. Weber, U. Wagner, M. O. Kurrer, J. Bremer, G. Iezzi, R. Graf, P. A. Clavien, R. Thimme, H. Blum, S. A. Nedospasov, K. Zatloukal, M. Ramzan, S. Ciesek, T. Pietschmann, P. N. Marche, M. Karin, M. Kopf, J. L. Browning, A. Aguzzi, and M. Heikenwalder. 2009. A lymphotoxin-driven pathway to hepatocellular carcinoma. *Cancer cell* 16:295-308.

92. Danese, S., A. Malesci, and S. Vetrano. Colitis-associated cancer: the dark side of inflammatory bowel disease. *Gut* 60:1609-1610.

93. Maeda, S., H. Kamata, J. L. Luo, H. Leffert, and M. Karin. 2005. IKKbeta couples hepatocyte death to cytokine-driven compensatory proliferation that promotes chemical hepatocarcinogenesis. *Cell* 121:977-990.

94. Greten, F. R., L. Eckmann, T. F. Greten, J. M. Park, Z. W. Li, L. J. Egan, M. F. Kagnoff, and M. Karin. 2004. IKKbeta links inflammation and tumorigenesis in a mouse model of colitis-associated cancer. *Cell* 118:285-296.

95. Takahashi, H., H. Ogata, R. Nishigaki, D. H. Broide, and M. Karin. 2010. Tobacco smoke promotes lung tumorigenesis by triggering IKKbeta- and JNK1-dependent inflammation. *Cancer cell* 17:89-97.

96. Pulendran, B., and R. Ahmed. 2011. Immunological mechanisms of vaccination. *Nature immunology* 131:509-517.

97. Kasturi, S. P., I. Skountzou, R. A. Albrecht, D. Koutsonanos, T. Hua, H. I. Nakaya, R. Ravindran, S. Stewart, M. Alam, M. Kwissa, F. Villinger, N. Murthy, J. Steel, J. Jacob, R. J. Hogan, A. Garcia-Sastre, R. Compans, and B. Pulendran. 2011. Programming the magnitude and persistence of antibody responses with innate immunity. *Nature* 470:543-547.

98. Honda, K., A. Takaoka, and T. Taniguchi. 2006. Type I inteferon gene induction by the interferon regulatory factor family of transcription factors. *Immunity* 25:349-360.

99. Harhaj, E. W., and V. M. Dixit. 2011. Deubiquitinases in the regulation of NF-kappaB signaling. *Cell research* 21:22-39.

100. Charoenthongtrakul, S., Q. Zhou, N. Shembade, N. S. Harhaj, and E. W. Harhaj. 2011. HTLV-I Tax inhibits innate antiviral signaling via NF-{kappa}B-dependent induction of SOCS1. *Journal of virology*.

101. Chan, G., E. R. Bivins-Smith, M. S. Smith, and A. D. Yurochko. 2008. Transcriptome analysis of NF-kappaB- and phosphatidylinositol 3-kinase-regulated genes in human cytomegalovirus-infected monocytes. *Journal of virology* 82:1040-1046.

102. Hayden, M. S., A. P. West, and S. Ghosh. 2006. NF-kappaB and the immune response. *Oncogene* 25:6758-6780.

103. Wang, J., S. H. Basagoudanavar, X. Wang, E. Hopewell, R. Albrecht, A. Garcia-Sastre, S. Balachandran, and A. A. Beg. 2010. NF-{kappa}B RelA Subunit Is Crucial for Early IFN-{beta} Expression and Resistance to RNA Virus Replication. *J Immunol*.

104. Hoffmann, A., and D. Baltimore. 2006. Circuitry of nuclear factor kappaB signaling. *Immunological reviews* 210:171-186.

105. Adli, M., E. Merkhofer, P. Cogswell, and A. S. Baldwin. 2010. IKKalpha and IKKbeta each function to regulate NF-kappaB activation in the TNF-induced/canonical pathway. *PloS one* 5:e9428.

106. Sun, S. C. 2011. Non-canonical NF-kappaB signaling pathway. *Cell research* 21:71-85.

107. Antonia, S. J., N. Mirza, I. Fricke, A. Chiappori, P. Thompson, N. Williams, G. Bepler, G. Simon, W. Janssen, J. H. Lee, K. Menander, S. Chada, and D. I. Gabrilovich. 2006. Combination of p53 cancer vaccine with chemotherapy in patients with extensive stage small cell lung cancer. *Clin Cancer Res* 12:878-887.

108. Ouaaz, F., J. Arron, Y. Zheng, Y. Choi, and A. A. Beg. 2002. Dendritic cell development and survival require distinct NF-kappaB subunits. *Immunity* 16:257-270.

109. Hunter, T. B., M. Alsarraj, R. P. Gladue, V. Bedian, and S. J. Antonia. 2007. An agonist antibody specific for CD40 induces dendritic cell maturation and promotes autologous anti-tumour T-cell responses in an in vitro mixed autologous tumour cell/lymph node cell model. *Scand J Immunol* 65:479-486.

110. Lugli E, R. M., Cossarizza A. 2010. Data analysis in flow cytometry: the future just started. *Cytometry A.* 77:705-713.

111. Valenzuela, J. O., C. Iclozan, M. S. Hossain, M. Prlic, E. Hopewell, C. C. Bronk, J. Wang, E. Celis, R. W. Engelman, B. R. Blazar, M. J. Bevan, E. K. Waller, X. Z. Yu, and A. A. Beg. 2009. PKCtheta is required for alloreactivity and GVHD but not for immune responses toward leukemia and infection in mice. *The Journal of clinical investigation* 119:3774-3786.

112. Liang, Y., C. Liu, J. Y. Djeu, B. Zhong, T. Peters, K. Scharffetter-Kochanek, C. Anasetti, and X. Z. Yu. 2007. {beta}2 integrins separates graft-versus-host disease and graft-versus-leukemia effect. *Blood* 111:954-962.

113. Nava-Parada, P., G. Forni, K. L. Knutson, L. R. Pease, and E. Celis. 2007. Peptide vaccine given with a Toll-like receptor agonist is effective for the treatment and prevention of spontaneous breast tumors. *Cancer research* 67:1326-1334.

114. Martin-Orozco, N., P. Muranski, Y. Chung, X. O. Yang, T. Yamazaki, S. Lu, P. Hwu, N. P. Restifo, W. W. Overwijk, and C. Dong. 2009. T helper 17 cells promote cytotoxic T cell activation in tumor immunity. *Immunity* 31:787-798.

115. Cho, H. I., Y. R. Lee, and E. Celis. 2011. Interferon gamma limits the effectiveness of melanoma peptide vaccines. *Blood* 117:135-144.

116. Gambotto, A., G. Dworacki, V. Cicinnati, T. Kenniston, J. Steitz, T. Tuting, P. D. Robbins, and A. B. DeLeo. 2000. Immunogenicity of enhanced green fluorescent protein (EGFP) in BALB/c mice: identification of an H2-Kd-restricted CTL epitope. *Gene therapy* 7:2036-2040.

117. Sadikot, R. T., W. Han, M. B. Everhart, O. Zoia, R. S. Peebles, E. D. Jansen, F. E. Yull, J. W. Christman, and T. S. Blackwell. 2003. Selective I kappa B kinase expression in airway epithelium generates neutrophilic lung inflammation. *J Immunol* 170:1091-1098.

118. Carlsen, H., J. O. Moskaug, S. H. Fromm, and R. Blomhoff. 2002. In vivo imaging of NF-kappa B activity. *J Immunol* 168:1441-1446.

119. Andreakos, E., R. O. Williams, J. Wales, B. M. Foxwell, and M. Feldmann. 2006. Activation of NF-kappaB by the intracellular expression of NF-kappaB-inducing kinase acts as a powerful vaccine adjuvant. *Proceedings of the National Academy of Sciences of the United States of America* 103:14459-14464.

120. Ruddle, N. H. 1999. Lymphoid neo-organogenesis: lymphotoxin's role in inflammation and development. *Immunologic research* 19:119-125.

121. Hoshino, K., T. Sugiyama, M. Matsumoto, T. Tanaka, M. Saito, H. Hemmi, O. Ohara, S. Akira, and T. Kaisho. 2006. IkappaB kinase-alpha is critical for interferon-alpha production induced by Toll-like receptors 7 and 9. *Nature* 440:949-953.

122. Wang, R. P., M. Zhang, Y. Li, F. C. Diao, D. Chen, Z. Zhai, and H. B. Shu. 2008. Differential regulation of IKK alpha-mediated activation of IRF3/7 by NIK. *Molecular immunology* 45:1926-1934.

123. Shinkura, R., K. Kitada, F. Matsuda, K. Tashiro, K. Ikuta, M. Suzuki, K. Kogishi, T. Serikawa, and T. Honjo. 1999. Alymphoplasia is caused by a point mutation in the mouse gene encoding Nf-kappa b-inducing kinase. *Nature genetics* 22:74-77.

124. Fagarasan, S., R. Shinkura, T. Kamata, F. Nogaki, K. Ikuta, K. Tashiro, and T. Honjo. 2000. Alymphoplasia (aly)-type nuclear factor kappaB-inducing kinase (NIK) causes defects in secondary lymphoid tissue chemokine receptor signaling and homing of peritoneal cells to the gut-associated lymphatic tissue system. *The Journal of experimental medicine* 191:1477-1486.

125. Karrer, U., A. Althage, B. Odermatt, H. Hengartner, and R. M. Zinkernagel. 2000. Immunodeficiency of alymphoplasia mice (aly/aly) in vivo: structural

defect of secondary lymphoid organs and functional B cell defect. *European journal of immunology* 30:2799-2807.

126. Joffre, O., M. A. Nolte, R. Sporri, and C. Reis e Sousa. 2009. Inflammatory signals in dendritic cell activation and the induction of adaptive immunity. *Immunological reviews* 227:234-247.

127. Dunn, G. P., A. T. Bruce, H. Ikeda, L. J. Old, and R. D. Schreiber. 2002. Cancer immunoediting: from immunosurveillance to tumor escape. *Nature immunology* 3:991-998.

128. Ouaaz, F., M. Li, and A. A. Beg. 1999. A critical role for the RelA subunit of nuclear factor kappaB in regulation of multiple immune-response genes and in Fas-induced cell death. *The Journal of experimental medicine* 189:999-1004.

129. Ben-Neriah, Y., and M. Karin. Inflammation meets cancer, with NF-kappaB as the matchmaker. *Nature immunology* 12:715-723.

130. Fridman, W. H., J. Galon, M. C. Dieu-Nosjean, I. Cremer, S. Fisson, D. Damotte, F. Pages, E. Tartour, and C. Sautes-Fridman. 2010. Immune Infiltration in Human Cancer: Prognostic Significance and Disease Control. *Current topics in microbiology and immunology*.

131. Pages, F., A. Berger, M. Camus, F. Sanchez-Cabo, A. Costes, R. Molidor, B. Mlecnik, A. Kirilovsky, M. Nilsson, D. Damotte, T. Meatchi, P. Bruneval, P. H. Cugnenc, Z. Trajanoski, W. H. Fridman, and J. Galon. 2005. Effector memory T cells, early metastasis, and survival in colorectal cancer. *The New England journal of medicine* 353:2654-2666.

132. Cho, H. I., and E. Celis. 2009. Optimized peptide vaccines eliciting extensive CD8 T-cell responses with therapeutic antitumor effects. *Cancer research* 69:9012-9019.

133. Torabian, S. Z., D. de Semir, M. Nosrati, S. Bagheri, A. A. Dar, S. Fong, Y. Liu, S. Federman, J. Simko, C. Haqq, R. J. Debs, and M. Kashani-Sabet. 2009. Ribozyme-mediated targeting of IkappaBgamma inhibits melanoma invasion and metastasis. *The American journal of pathology* 174:1009-1016.

134. Cho, H. I., G. Niu, N. Bradley, and E. Celis. 2008. Optimized DNA vaccines to specifically induce therapeutic CD8 T cell responses against autochthonous breast tumors. *Cancer Immunol Immunother* 57:1695-1703.

135. Van Gelder, R. N., M. E. von Zastrow, A. Yool, W. C. Dement, J. D. Barchas, and J. H. Eberwine. 1990. Amplified RNA synthesized from

limited quantities of heterogeneous cDNA. *Proceedings of the National Academy of Sciences of the United States of America* 87:1663-1667.

136. Warrington, J. A., A. Nair, M. Mahadevappa, and M. Tsyganskaya. 2000. Comparison of human adult and fetal expression and identification of 535 housekeeping/maintenance genes. *Physiological genomics* 2:143-147.

137. Meylan, E., A. L. Dooley, D. M. Feldser, L. Shen, E. Turk, C. Ouyang, and T. Jacks. 2009. Requirement for NF-kappaB signalling in a mouse model of lung adenocarcinoma. *Nature* 462:104-107.

138. Assudani, D., H. I. Cho, N. DeVito, N. Bradley, and E. Celis. 2008. In vivo expansion, persistence, and function of peptide vaccine-induced CD8 T cells occur independently of CD4 T cells. *Cancer research* 68:9892-9899.

139. Baggiolini, M. 1998. Chemokines and leukocyte traffic. *Nature* 392:565-568.

140. Loberg, R. D., C. Ying, M. Craig, L. Yan, L. A. Snyder, and K. J. Pienta. 2007. CCL2 as an important mediator of prostate cancer growth in vivo through the regulation of macrophage infiltration. *Neoplasia* 9:556-562.

141. Stathopoulos, G. T., T. P. Sherrill, W. Han, R. T. Sadikot, F. E. Yull, T. S. Blackwell, and B. Fingleton. 2008. Host nuclear factor-kappaB activation potentiates lung cancer metastasis. *Mol Cancer Res* 6:364-371.

142. Berencsi, K., P. Rani, T. Zhang, L. Gross, M. Mastrangelo, N. J. Meropol, D. Herlyn, and R. Somasundaram. 2011. In vitro migration of cytotoxic T lymphocyte derived from a colon carcinoma patient is dependent on CCL2 and CCR2. *Journal of translational medicine* 9:33.

143. Sadofsky, M. J. 2004. Recombination-activating gene proteins: more regulation, please. *Immunological reviews* 200:83-89.

144. Flanagan, S. P. 1966. 'Nude', a new hairless gene with pleiotropic effects in the mouse. *Genetical research* 8:295-309.

145. Budzynski, W., and C. Radzikowski. 1994. Cytotoxic cells in immunodeficient athymic mice. *Immunopharmacology and immunotoxicology* 16:319-346.

146. Shinkai, Y., G. Rathbun, K. P. Lam, E. M. Oltz, V. Stewart, M. Mendelsohn, J. Charron, M. Datta, F. Young, A. M. Stall, and et al. 1992. RAG-2-deficient mice lack mature lymphocytes owing to inability to initiate V(D)J rearrangement. *Cell* 68:855-867.

147. Karin, M., and F. R. Greten. 2005. NF-kappaB: linking inflammation and immunity to cancer development and progression. *Nature reviews* 5:749-759.

148. Karin, M., Y. Yamamoto, and Q. M. Wang. 2004. The IKK NF-kappa B system: a treasure trove for drug development. *Nat Rev Drug Discov* 3:17-26.